FIELD TESTING OF DRILLED SHAFTS TO DEVELOP DESIGN METHODS

Lymon C. Reese
W. Ronald Hudson

Research Report Number 89-1

Soil Properties as Related to Load Transfer
Characteristics in Drilled Shafts

Research Project 3-5-65-89

conducted for

The Texas Highway Department

in cooperation with the
U. S. Department of Transportation
Federal Highway Administration
Bureau of Public Roads

by the

CENTER FOR HIGHWAY RESEARCH
THE UNIVERSITY OF TEXAS AT AUSTIN

April 1968

The opinions, findings, and conclusions expressed in this publication are those of the authors and not necessarily those of the Bureau of Public Roads.

PREFACE

This, the first in a series of reports from Research Project 3-5-65-89 of the Cooperative Highway Research Program, describes the overall approach to the design of drilled shafts based on a series of field and laboratory investigations. Subsequent reports will give specific details and findings of the various phases including results of field load tests, and in time a report will be submitted with design recommendations in final form.

This report is the product of the combined efforts of many people. Technical contributions were made by Harold H. Dalrymple, James N. Anagnos, Crozier Brown, Clarence Ehlers, John W. Chuang, V. N. Vijayvergiya, and Mike O'Neill. Preparation and editing of the manuscript were done by Art Frakes, Joye Linkous, and Don Fenner.

The Texas Highway Department Project Contact Representatives Messrs. Horace Hoy and H. D. Butler and District No. 14 personnel have been helpful and cooperative in the development of the work. Thanks are due them as well as the U. S. Bureau of Public Roads who jointly sponsored the work.

Lymon C. Reese
W. Ronald Hudson

April 1968

ABSTRACT

Drilled shafts are important foundation elements with many purposes, but they are used primarily to resist axial loads. A plan of research is described here to investigate the load carrying capacity of such shafts by field tests, including the following important steps:

(1) developing instrumentation to obtain information on the interaction of the soil and shaft,

(2) performing load tests on a full-scale drilled shaft,

(3) determining soil properties,

(4) using field and laboratory tests to develop a theory of drilled shaft behavior,

(5) running additional field tests to verify the theory, and

(6) translating the theory into a procedure for design.

A general description is given of some preliminary tests conducted at a site in Austin, Texas; development of instrumentation and instrumentation problems are discussed; a preliminary method of evaluating soil strength, including the interaction of the soil and wet concrete, is presented; and a technique for applying this information to design is discussed.

A preliminary design method which combines all the information developed to date is presented for further study.

TABLE OF CONTENTS

NOMENCLATURE

Symbol	Typical Units	Definition
A	sq ft	Cross-sectional area of shaft
c	lbs/sq ft	Apparent cohesion of soil
c_i	lbs/sq ft	Shearing resistance of undisturbed soil at i^{th} increment
C	ft	Circumference of shaft
E	lbs/sq ft	Young's modulus of shaft material
h	ft	Increment length of shaft in finite difference equations
i	-	Subscript which denotes a general station number or increment
m	-	Station number of point on shaft in finite difference equations
M	-	Number of increments in shaft
N_c	-	Bearing-capacity factor
Q_z	lbs	Total load in shaft at a point z below top of shaft
Q_B	lbs	Bottom load on shaft
Q_T	lbs	Total load on top of shaft
R	lbs	Total peripheral load on shaft
s_z	lbs/sq ft	Load transfer at a point z below top of shaft
w	percent	Moisture content
w_s	ft	Compression in shaft due to load
w_z	ft	Vertical movement of shaft at point z

Symbol	Typical Units	Definition
w_B	ft	Vertical movement at bottom of shaft
w_T	ft	Total vertical movement of top of shaft
y_z	ft	Vertical coordinate from ground surface to a point in the shaft
z	ft	Vertical coordinate from top of the shaft to a point in the shaft
α	-	Shearing resistance modification factor
β_z	lb/cu ft	Function which relates s_z to w_z
ΔA_i	sq ft	Peripheral area of shaft at i^{th} increment
ΔR_i	lb	Shaft side resistance at i^{th} increment
η	ft/lb	$\frac{C}{EA}$
σ	lbs/sq ft	Normal stress
τ	lbs/sq ft	Shearing stress
ϕ	degrees	Apparent angle of internal friction of soil

CHAPTER 1. INTRODUCTION

This report deals with a research program aimed at developing a better understanding of the behavior of drilled shafts. While the term "drilled shaft" is familiar to most readers, some clarification is useful. Figure 1 shows a typical drilled shaft foundation element. The construction procedure includes: (1) drilling a hole, with or without a bell being cut, depending on the soil condition at the site and on the proposed use of the shaft; (2) inspecting the drilled hole; (3) placing reinforcing steel; and (4) concreting.

When deep foundations are required, drilled shafts are often specified if the site conditions permit the hole to stand open or to be economically cased. The subsequent inspection and construction operations are greatly facilitated in such cases, but there are numerous instances when drilled shafts have successfully been installed where water was present. The water may be sealed off, the water table may be lowered, or drilling mud may be used to keep the hole open.

The research program described here is restricted to the study of the drilled shaft under axial load only, although such foundations could readily be designed to resist inclined and eccentric loads. While the case of a shaft constructed by pouring tremie concrete into a hole filled with a slurry is not completely excluded from this study, a shaft poured into a relatively dry hole is of principal interest. The general intention of the program is to develop a good understanding of the interaction of a drilled shaft with the supporting soil, with the specific aim of developing criteria leading to a more economic, secure design.

Several different procedures are presently used in the design of drilled shafts: (1) load is frequently assumed to be transmitted through point-bearing only; (2) the design load is computed from the results of the Texas Highway Department cone penetrometer tests or from the results of soil shear-strength tests; or (3) if side resistance is assumed, the load transfer is usually computed using a reduced shear strength of the soil along the sides of the shaft.

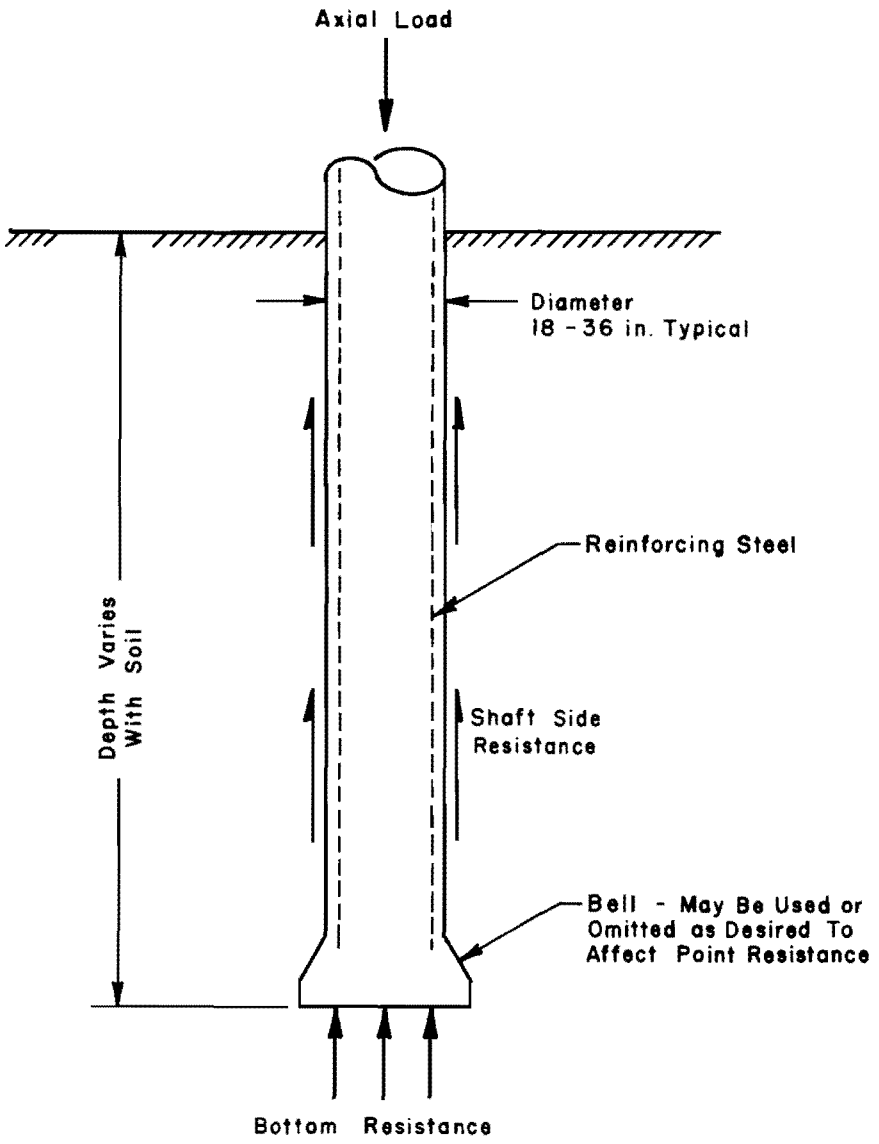

Fig 1. Sketch of a typical drilled shaft.

Because of the lack of data concerning the interaction of a drilled shaft with the supporting soil, particularly data obtained from full-scale load tests, no design procedure is presently available which treats rationally all the significant parameters in the drilled shaft problem.

In view of the large number of drilled shafts used by the Texas Highway Department, a research program was initiated at the Center for Highway Research, The University of Texas, on the drilled shaft problem. This report presents the plan for this program as well as some of the early results.

The general research plan involves the following steps:

(1) developing instrumentation capable of yielding data to provide information on the interaction of full-scale drilled shafts with the supporting soil,

(2) performing a series of load tests on full-scale drilled shafts,

(3) determining significant soil properties at the field sites, using appropriate field and laboratory tests,

(4) using results of field load tests, along with results of laboratory tests, to develop a theory for the behavior of drilled shafts,

(5) running additional field load tests, on instrumented or uninstrumented shafts, as needed to verify the theory, and

(6) translating the theory into a procedure suitable for use by designers.

CHAPTER 2. LOAD TRANSFER IN DRILLED SHAFTS

Mechanics of Load Transfer

While the mechanics of load transfer from a drilled shaft to the supporting soil is not well understood and is the subject of this investigation, some general aspects of the mechanics are known and presented here to clarify the research goals.

A typical load-settlement curve for drilled shafts is shown in Fig 2. The vertical dashed line in the figure is the load which causes plunging, that is, the load which will cause continued settlement of the shaft with no increase in load. If the load is increased to some value Q_p at point P, the gross settlement is represented by the horizontal dashed line to point P. If the load is then released, there is some rebound as indicated by the light solid line, with the net settlement being defined as the settlement at zero load after unloading. The manner in which the load is distributed from the drilled shaft to the supporting soil is of interest. A typical curve of the distribution of load along the length of an axially loaded drilled shaft is shown in Fig 3. The slope of the curve indicates the rate of load transfer from the drilled shaft to the soil.

Some insight into the problem of the mechanics of load transfer from a drilled shaft may be obtained by considering the idealized load-distribution and load-settlement curves in Fig 4 (Ref 1). Figure 4(a) shows the results of loading a shaft which rests on an unyielding surface in which all the load is transferred by tip resistance and none by side resistance. The load-distribution curves for loads of Q_{T_1} and Q_{T_2} show a constant load in the shaft regardless of depth. The load-settlement curve for such a case is also shown. The settlement, or movement at the top of the shaft, can be obtained by computing the compression in the shaft from basic principles of mechanics. The load-settlement curve will be a straight line, as shown, if the effective modulus of elasticity of the shaft is linear.

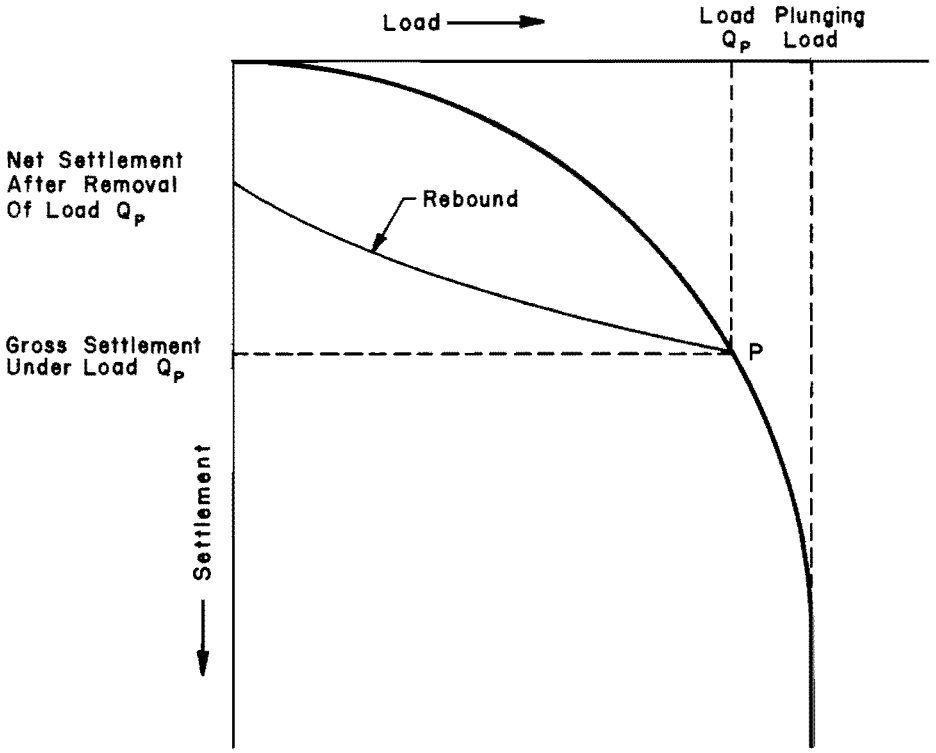

Fig 2. Typical load-settlement curve.

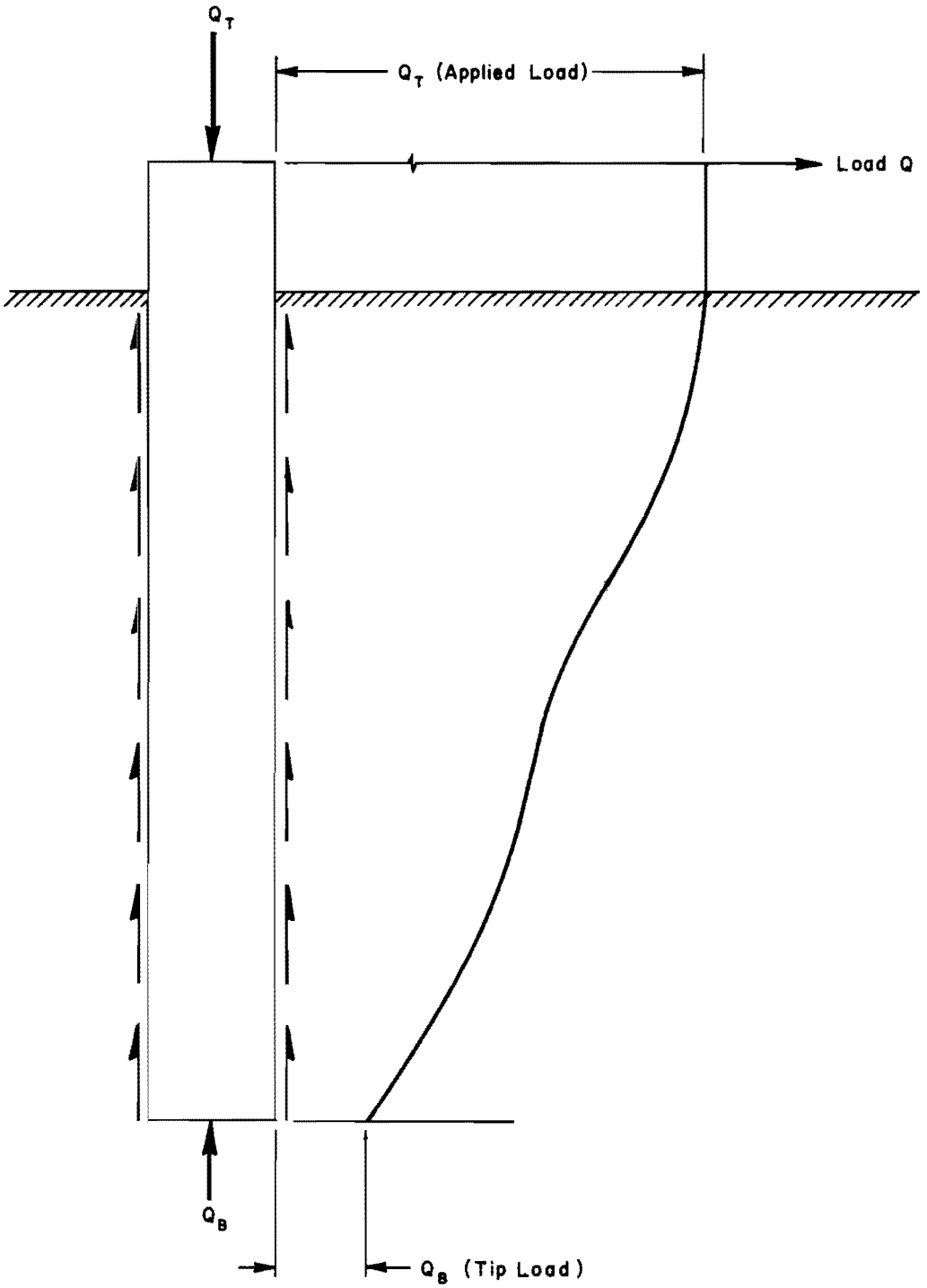

Fig 3. Curve showing typical distribution of load along the length of an axially loaded drilled shaft.

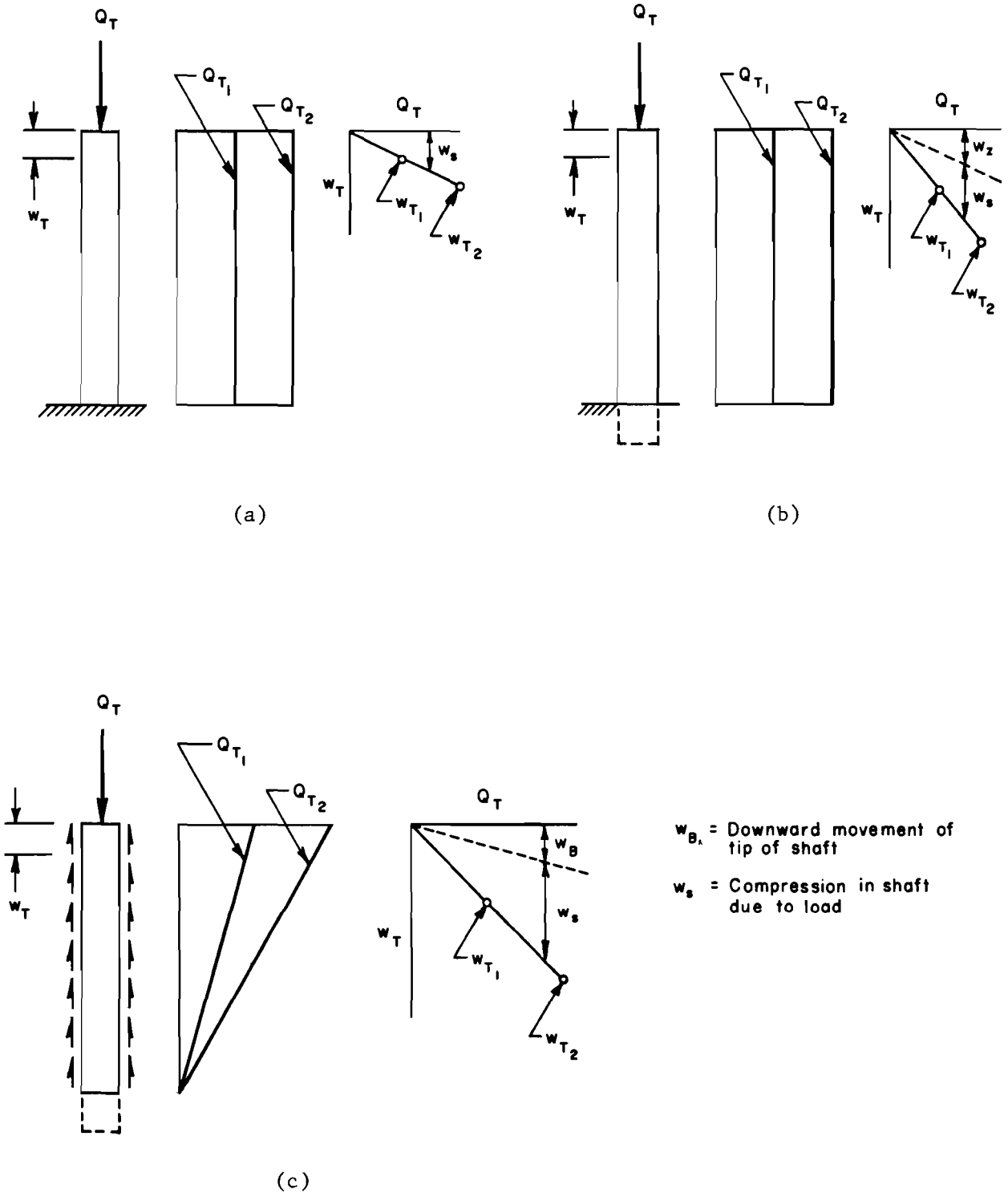

Fig 4. Idealized load-distribution and load-settlement curves for an axially loaded drilled shaft.

Figure 4(b) shows a similar shaft but in this instance its tip is assumed to be resting on an elastic surface which yields linearly with the applied load. The load-distribution curves remain unchanged, as shown. However, the settlement of the top of the shaft is now made up of two quantities: (1) compression in the shaft due to the applied load and (2) the settlement of the shaft tip.

Figure 4(c) shows the case where the soil produces a uniform shaft resistance with no tip resistance. The load-distribution curves are triangular, as indicated. The load settlement is again linear and made up of the compression in the shaft due to the triangular distribution of load, and the settlement of the tip of the shaft.

While of interest, none of these idealized models represents the true behavior of the axially loaded drilled shaft. A real shaft has some combination of all these factors plus nonuniform and nonlinear behavior. A more realistic model is shown in Fig 5. Figure 5(a) shows the free body of a drilled shaft in peripheral equilibrium where the applied load Q_T is balanced by a tip load Q_B plus side loads R. A mechanism is shown in Fig 5(b) which can be used to illustrate the deformations in the drilled shaft. The shaft has been replaced by an elastic spring. Representing the soil is a set of nonlinear springs spaced along the shaft, with one spring depicting the soil behavior beneath the shaft tip. The ordinate s_z of the curves is load transfer and the abscissa w_z is the shaft movement. No load is transferred from shaft to soil unless there is a downward movement of the shaft. This downward movement is dependent on the applied load, on the position along the shaft, on the stress-strain characteristics of the shaft material, and on the load transfer-movement curves along the shaft and at the shaft tip. To solve the problem of the distribution of load along the shaft for a given applied load, along with the determination of downward movement at any point along the shaft, a nonlinear differential equation must be solved.

The differential equation can be obtained by considering an element from the shaft as shown in Fig 6 (Ref 2). The unit strain is

$$\frac{dw_z}{dz} = \frac{Q_z}{EA} \qquad (1)$$

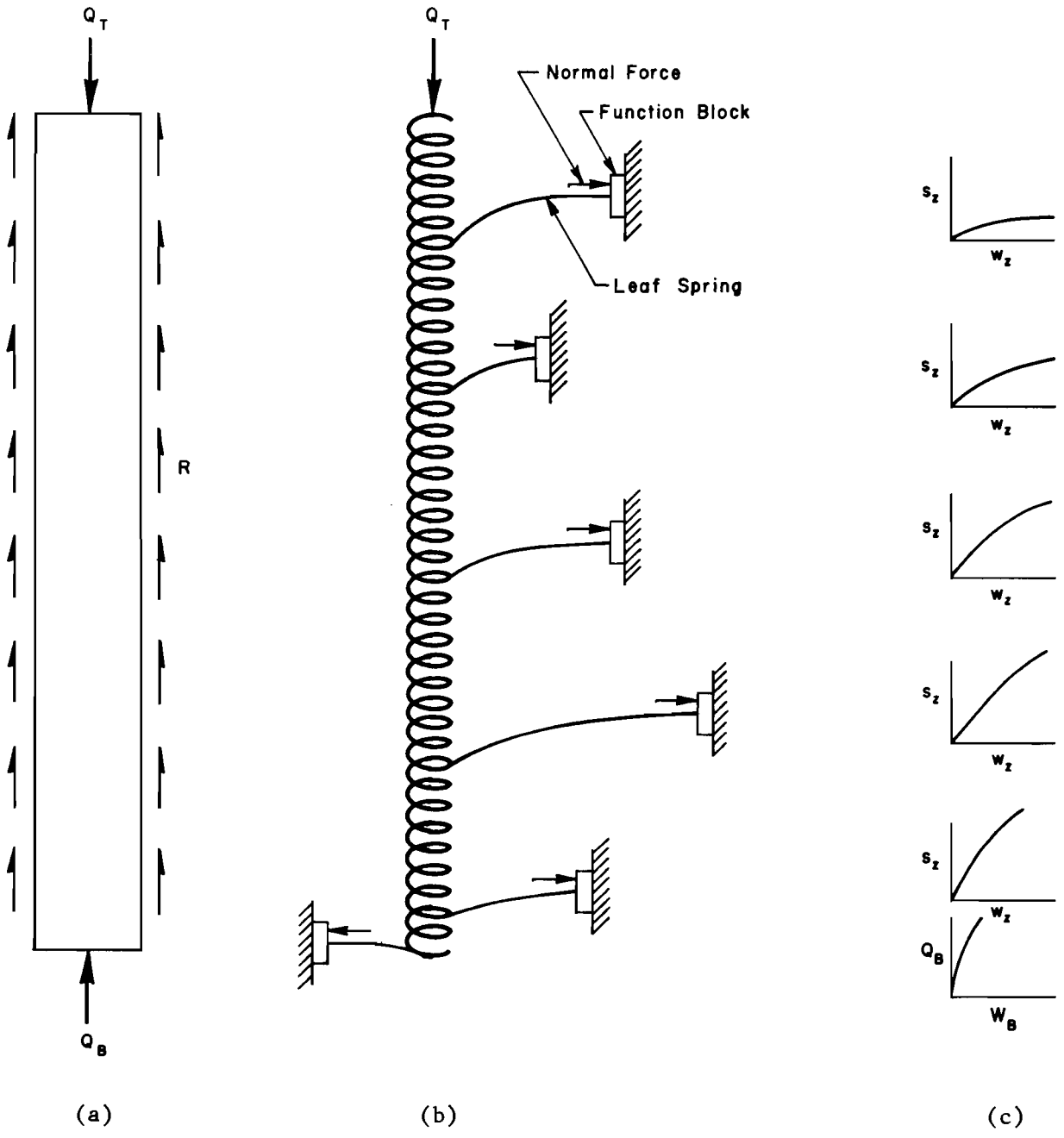

Fig 5. Mechanical model of axially loaded drilled shaft.

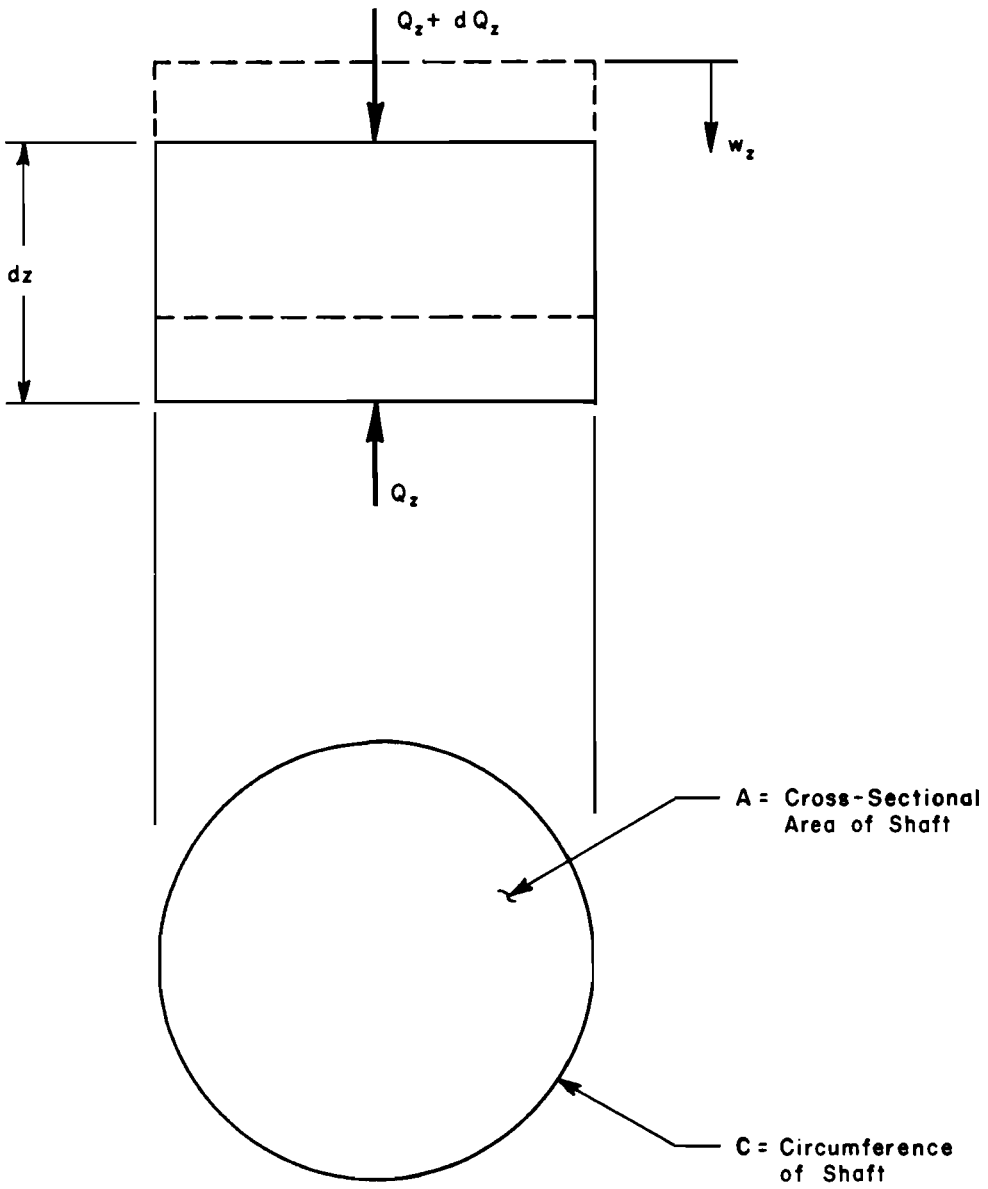

Fig 6. Element from an axially loaded shaft.

where

E = modulus of elasticity of the shaft material,

A = cross-sectional area of the shaft,

Q_z = total load in the shaft at point z,

w_z = vertical movement of the shaft at point z.

From Eq 1

$$Q_z = EA \frac{dw_z}{dz} . \tag{2}$$

Differentiating Eq 2 with respect to z,

$$\frac{dQ_z}{dz} = EA \frac{d^2w_z}{dz^2} . \tag{3}$$

If the load transfer from the shaft to the soil at point z, in force per unit of area, is defined as s_z, then

$$dQ_z = s_z C dz \tag{4}$$

where

C = circumference of the shaft at point z,

and

$$\frac{dQ_z}{dz} = s_z C . \tag{5}$$

Solving Eqs 3 and 5 simultaneously,

$$EA \frac{d^2w_z}{dz^2} = s_z C . \tag{6}$$

The load transfer can be expressed as a function of the shaft movement w_z, as follows:

$$s_z = \beta_z w_z \tag{7}$$

where

β_z = a function which depends on depth z and shaft movement w_z.

Equation 7 is substituted into Eq 6 to obtain the desired differential equation

$$\frac{d^2 w_z}{dz^2} - \eta \beta_z w_z = 0 \tag{8}$$

where

$$\eta = \frac{C}{EA} . \tag{9}$$

If η and β are constants, a closed-form solution can be obtained for Eq 8. However, since β cannot normally be a constant, the closed-form solution is of little importance and will not be presented.

Referring to Fig 7, a convenient solution to the nonlinear differential equation, Eq 8, is obtained by writing the equation in finite-difference form and using numerical techniques. Equation 8 becomes

$$\frac{\left(\frac{\Delta w_z}{\Delta z}\right)_{m+1} - \left(\frac{\Delta w_z}{\Delta z}\right)_{m-1}}{2h} = \eta \beta_m w_m . \tag{10}$$

Equation 1 can also be written in difference form as

$$\left(\frac{\Delta w_z}{\Delta z}\right)_i = \frac{Q_i}{(EA)_i} . \tag{11}$$

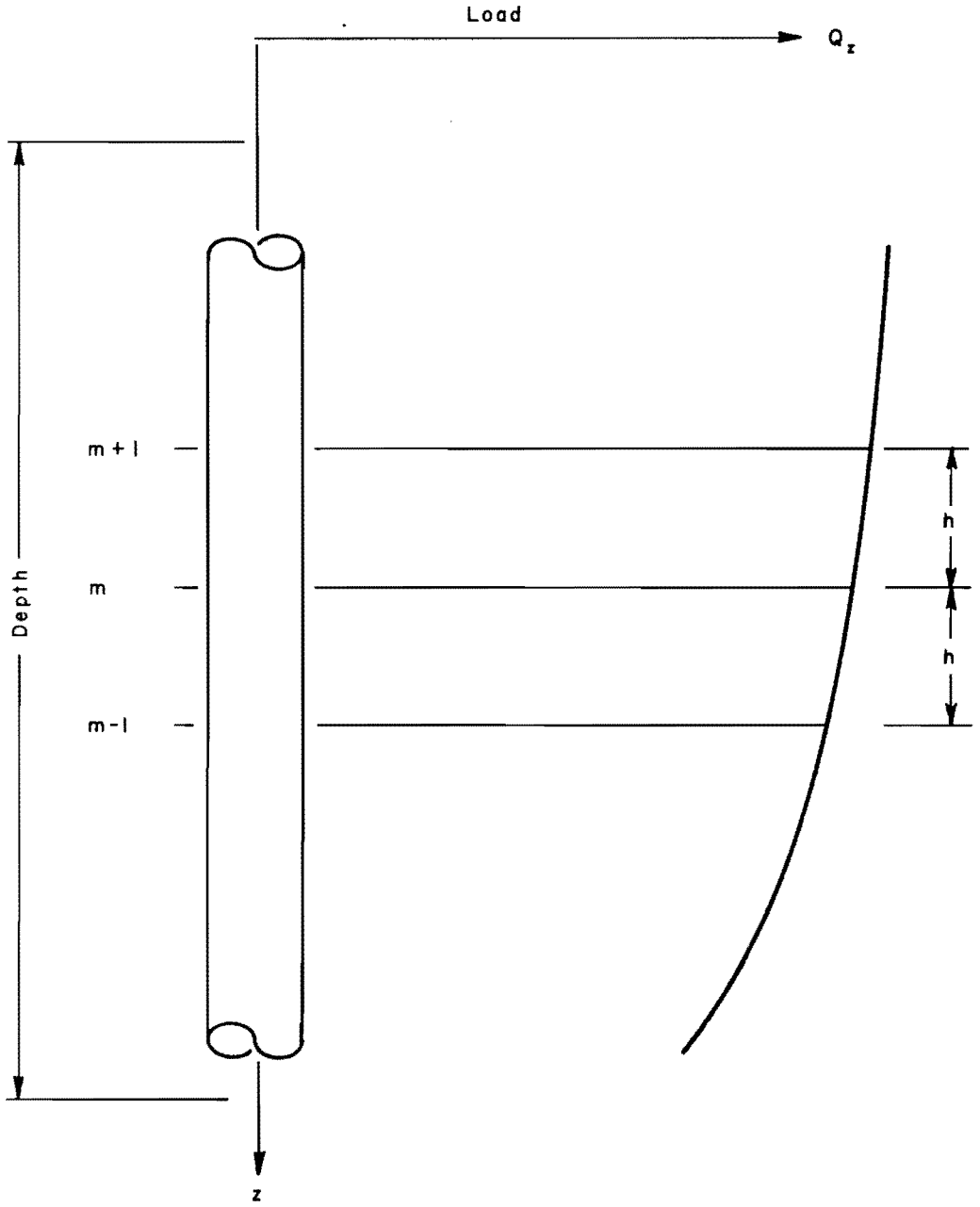

Fig 7. Segment of a load-distribution curve along an axially loaded drilled shaft.

Substituting the expressions from Eqs 11 and 9 into Eq 10, the following expression is obtained assuming a constant EA:

$$Q_{m+1} - Q_{m-1} = 2hC\beta_m w_m \quad . \tag{12}$$

Equations 11 and 12 are elementary, of course, but are sufficient to give a solution to the problem of the axially loaded drilled shaft.

Assuming that curves are available showing load transfer as a function of shaft movement, a suggested procedure for computing the load-settlement curve and a family of load-distribution curves can be developed as follows:

(1) Assume a slight downward movement of the shaft tip, refer to the corresponding load transfer curve, and obtain the resulting load on the shaft tip.

(2) Select the number of segments into which the shaft is to be divided (some experimenting will indicate the number required for acceptable accuracy) and consider the behavior of the bottom segment.

(3) Assume a load at the top of the bottom segment and compute the elastic compression in that segment, using Eq 11 written for that location.

(4) Use the assumed tip movement and the results of the computation in Step 3 to compute the downward movement at the midheight of the bottom segment.

(5) Refer to the appropriate curve showing load transfer versus shaft movement and obtain the resulting load transfer.

(6) Use the appropriate modification of Eq 12 and compute the load at the top of the bottom segment.

(7) Repeat Steps 3 through 6 until convergence is achieved.

(8) Compute, in a like manner, shaft loads and movements for the other segments until the top of the shaft is reached. This will yield one point on the load-settlement curve and one of the family of load-distribution curves.

(9) Select other assumed tip movements and repeat computations to produce the entire load-settlement curve and the whole family of load-distribution curves.

This outlined procedure has been used successfully as described in technical literature (Refs 1 through 4), and limitations on use of the method involve the accuracy with which load transfer curves can be predicted. Thus, one of the principal aims of the research reported here is the further development of methods of predicting load transfer curves for drilled shafts.

Experimental Techniques for Obtaining Load Transfer Curves

After the completion of a field load test on an instrumented drilled shaft, the curves shown in Figs 8(a) and 8(b) should be available. Figure 8(a) shows a load-settlement curve for the top of the drilled shaft. This curve may be obtained by measuring both the load with a load cell and the downward movement of the top of the shaft with dial gages. Figure 8(b) shows a set of curves which gives load in the drilled shaft at various points along its length for each of the applied loads. These data are obtained from instrumentation within the shaft. Such instrumentation is described in Chap 4 of this report. Figures 8(a) and 8(b) indicate that four loads were applied to the drilled shaft; however, in the general case, several more loads would have been applied.

From the data in Figs 8(a) and 8(b), it is desired to produce a set of load-transfer curves such as are shown in Fig 8(d). Such curves can be produced for any desired depth. Figure 8(c) illustrates the procedure for obtaining a point on one of the curves.

In this instance, the procedure for obtaining a point on one of the curves at a depth y_z below the ground surface is illustrated. For a particular load-distribution curve, corresponding to a particular load Q_z, the slope of the load-distribution curve is obtained at point y_z. In Fig 8(c) this slope is indicated as the quantity $\Delta Q_z/\Delta y_z$. To obtain the load transfer s_z, the quantity is then divided by the shaft circumference at the point y_z. Thus, the load transfer s_z normally would have the units pounds per square foot.

The downward movement of the shaft corresponding to the computed load transfer may be obtained as follows: (1) the settlement corresponding to the particular load in question is obtained from the curve 8(a); (2) the shortening of the shaft is computed by dividing the cross-hatched area, shown in Fig 8(c), by the shaft cross-sectional area times an effective modulus of elasticity; and (3) the downward movement of the shaft at point y_z is then computed by subtracting the shortening of the shaft from the observed settlement.

The above procedure enables one point on one load transfer curve to be obtained. In the same manner load transfer curves can be developed at the desired depths (see Fig 8(d)).

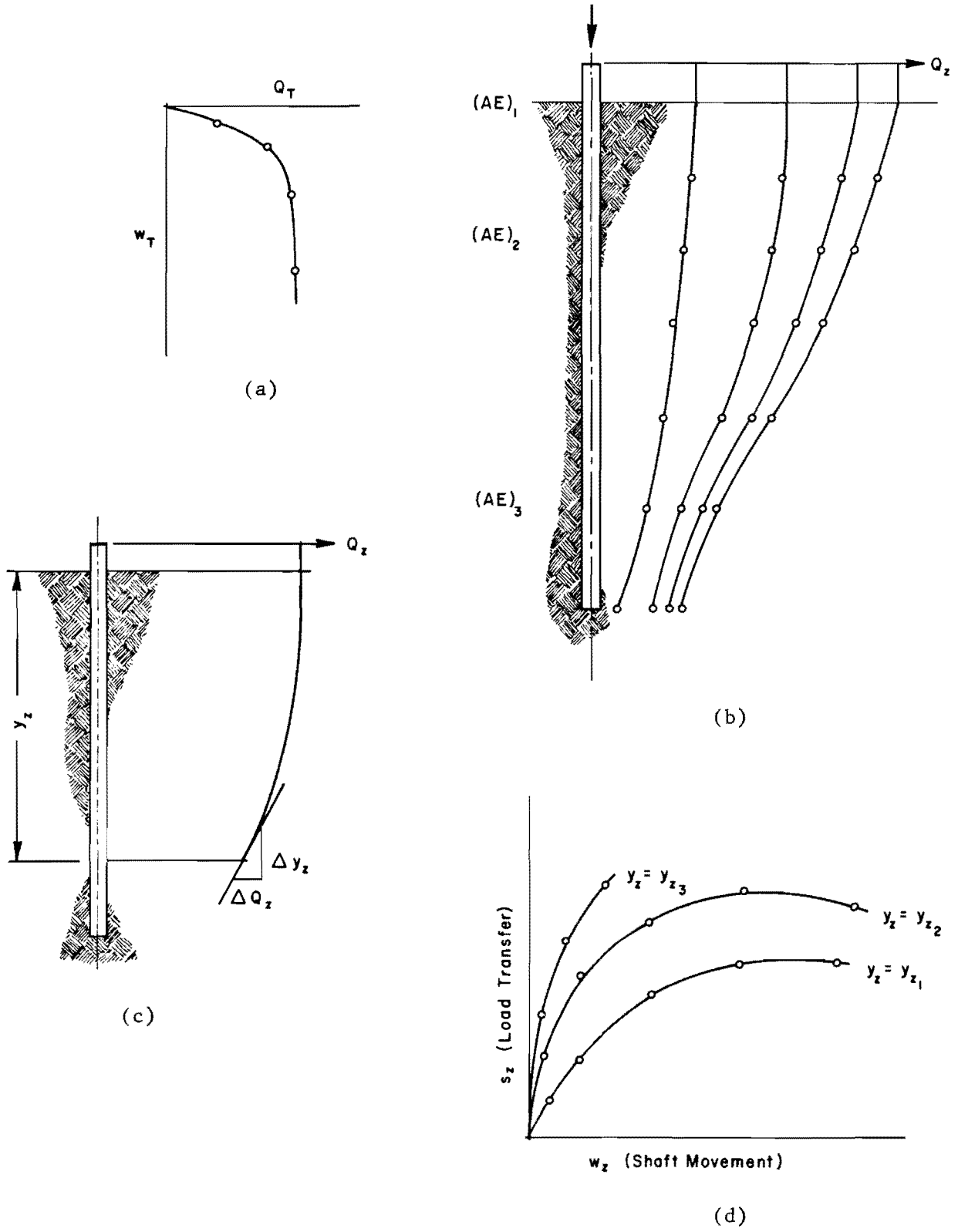

Fig 8. Development of load transfer versus movement curves.

As can be readily understood, accurate load-settlement and load-distribution data are required.

CHAPTER 3. SOILS STUDY

Site Investigation

In order to develop a design procedure for drilled shafts, correlations between the soil properties and load transfer curves must be evolved. The preceding sections have presented information on the development of load-transfer curves. Some of the aspects of the work on soil studies can be illustrated by referring to Fig 9 which shows a possible rupture line for soil plotted on a Mohr-Coulomb diagram. The rupture line is assumed to be straight over the range of interest and is assumed to be defined by an apparent cohesion c and an apparent angle of internal friction ϕ. Also shown on the plot is a dashed curve which indicates the possible ultimate values from a set of load transfer curves for a drilled shaft. The dashed curve indicates that for low values of normal pressure σ between the concrete and the soil, only a fraction of the shear strength is mobilized, and for higher values of normal pressure, all of the soil shear strength is mobilized.

The information in Fig 9 is speculative, of course, but the parameters which must be investigated are identified. At any given test location, the shear strength of the soil for each of the significant strata must be investigated and a rupture line determined as indicated in Fig 9. In addition, other important soil properties must be determined. In this connection, it will be important to know whether or not there is a change in the soil properties as a result of casting the drilled shaft and as a result of the passage of time.

At each site soil borings should be made and undisturbed soil samples should be obtained using thin-walled tubing. The samples should then be carefully extracted from the tube, enclosed in protective coverings, and transported to the laboratory for storage in humid rooms until testing. Depending on the nature of the samples, shear-strength tests are performed, perhaps including unconfined compression testing, triaxial compression testing, or direct shear testing. Other physical characteristics of the soil should also be determined, including density, natural water content, grain-size distribution, and Atterberg limits.

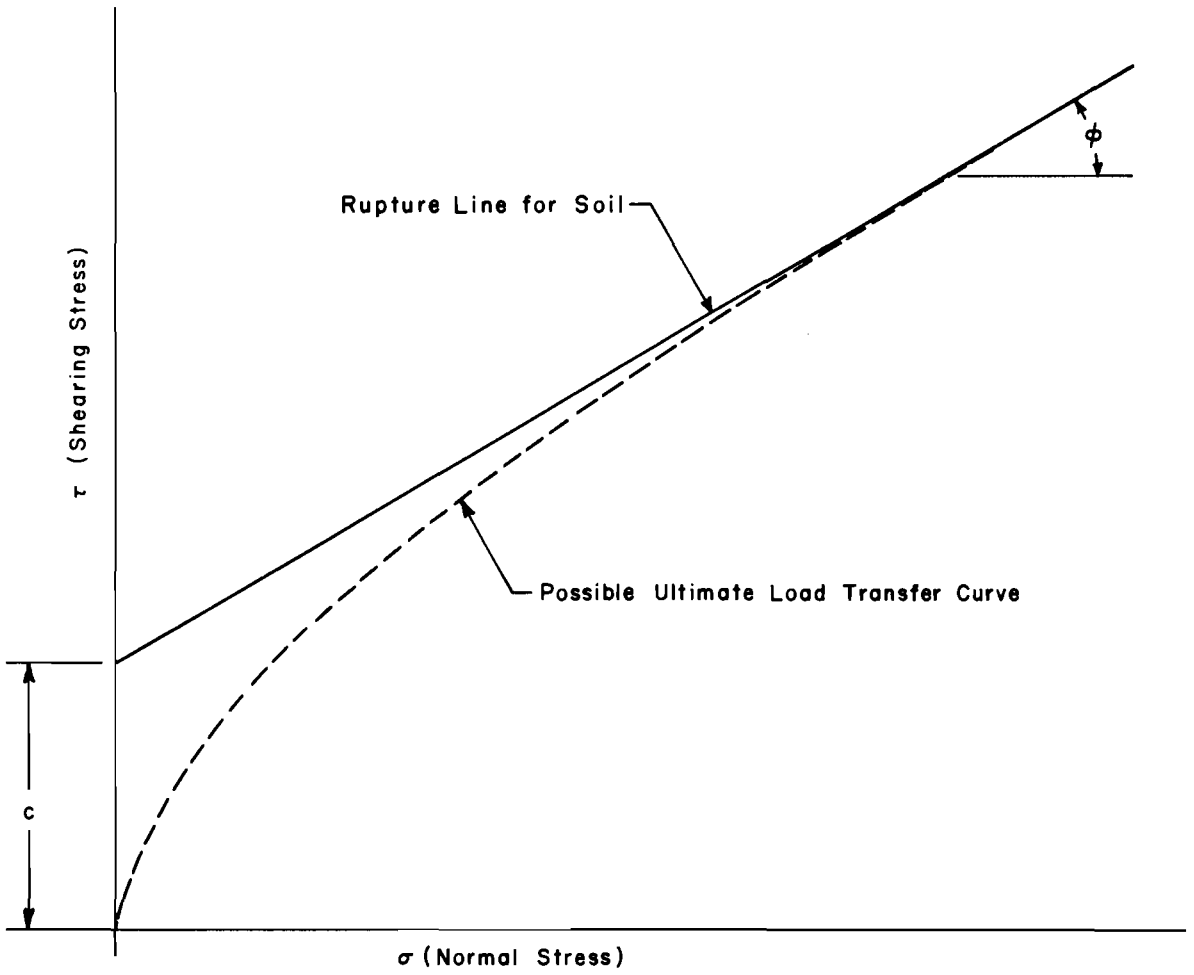

c = Apparent Cohesion

ϕ = Apparent Angle of Internal Friction

Fig 9. Load transfer related to soil shear strength.

Soil studies at the site, in addition to undisturbed sampling and laboratory testing, should include certain field tests, in particular, the cone penetrometer test employed by the Texas Highway Department. Empirical correlations can possibly be made with the results of penetrometer tests.

Along with investigations of the soil characteristics and their changes, studies must be undertaken to determine the specific mechanism of load transfer to the supporting soil. Specifically, the influence of the normal pressure between the drilled shaft and the supporting soil should be investigated.

In order to study the possible shift of the rupture line, because of interaction of the soil with wet concrete, and in order to gain some insight into the relationship between the load transfer curve and the rupture line, as indicated by the dashed line in Fig 9, the laboratory experiments described in the next section were performed.

Interaction Between Fresh Concrete and Soil

A series of laboratory experiments have been performed to examine the interaction between fresh concrete and soil. Figure 10 illustrates the device used, a special direct shear box developed so that soil, either a laboratory compacted soil or an undisturbed sample, can be placed in the bottom of the box, and the top of the box can then receive fresh concrete. Normal pressure can be applied to the fresh concrete to simulate the effect of overburden. After the fresh concrete has set, a shear test can be conducted. The failure plane can be controlled by adjusting the position of the joint between the two halves of the box.

Shearing resistance is determined at the interface between the concrete and the soil and at two positions in the soil sample. In addition, direct shear tests are performed on undisturbed soil for comparison.

In the soil sample at the interface between the soil and the concrete and at varying distances from this interface, water content measurements are made which are compared with the water content of the soil prior to testing.

The laboratory tests thus far show that there is normally a migration of water from the fresh concrete into the soil which results in the softening of the soil at the interface. In some instances, some migration of cement from the fresh concrete into the soil occurs. The water migration and the subsequent reduction in shear strength of the soil were influenced by the following

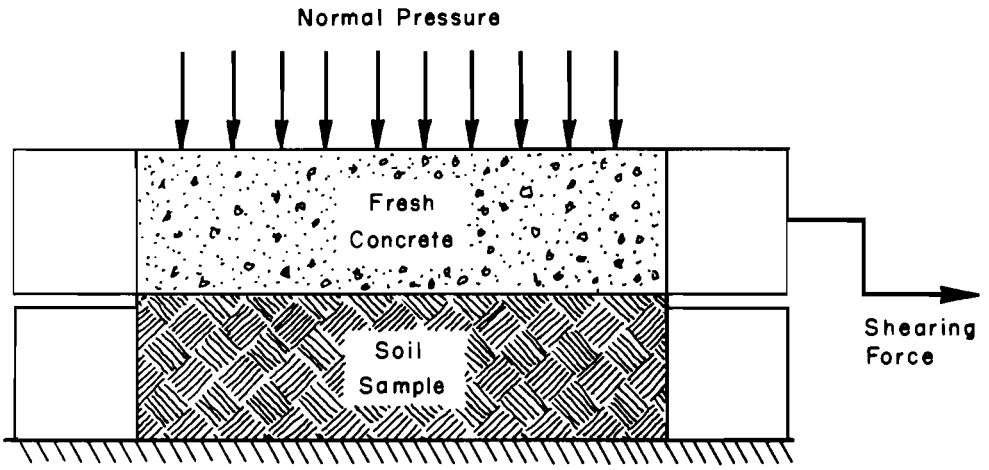

Fig 10. Laboratory direct shear box used in studying interaction of fresh concrete with soil.

parameters: pressure at the interface, the water-cement ration of the fresh concrete, the initial water content of the soil, and the nature of the soil.

Another report is being prepared giving the details of methods of analysis which will reveal the change in shear strength due to the interaction of the soil with fresh concrete. The experimental procedure to be recommended as a part of these methods may be described briefly as follows:

(1) Use thin-walled sampling tubes and obtain undisturbed samples down to the desired depth (some distance below the shaft tip).

(2) Consider the shaft to be composed of finite increments. Determine the shearing resistance and moisture content of the undisturbed soil at the level of each increment.

(3) Conduct tests to obtain the moisture migration from mortar to soil as a function of the overburden, using the undisturbed samples. The pressure between the mortar and soil may be determined by using equations developed for the pressure of fresh concrete against formwork.

(4) Use undisturbed soils with mortar-soil specimens to perform direct shear tests to determine shearing resistance. The shearing surface is forced to occur at the interface and in the soil at various distances from the interface. The value α is defined as the shearing resistance at a particular point divided by the shearing strength of the undisturbed soil.

(5) Plot soil moisture content versus distance from the interface for the various depths (from the results of Step 3).

(6) Plot from Step 4 α versus distance from the interface for the various depths. From this relationship determine the minimum values of α and the distance from the interface at which it occurs and thereby obtain the position of the weakest zone at each increment along the drilled shaft. The soil will fail along this zone.

(7) Obtain the modified shearing resistance of the soil after the concrete is poured by multiplying the value of shearing resistance of the undisturbed soil by the factor α .

The use of this procedure as a preliminary design approach is described in Chapter 6.

CHAPTER 4. DEVELOPMENT OF INSTRUMENTATION

The development of instrumentation for use in field experiments was an important part of the preliminary work on this research project. Of primary importance was instrumentation to determine the axial load in the drilled shaft with respect to depth. As indicated by the previous section, it was also important to know the lateral pressure between the concrete and the soil at the time of casting. Instrumentation which readily determined the moisture content of the soil as a function of depth was also needed.

Axial-Load Measurements

The devices shown in Fig 11 have been employed to determine the axial load in a drilled shaft. Figure 11(a) illustrates the use of "tell-tales," unstrained rods which are placed at various depths within the drilled shaft. During loading, the compression in the drilled shaft over the respective lengths of the rod is determined by use of ten-thousandth dial gages. These measurements, along with a knowledge of the deformation characteristics of the material in the shaft, are used to determine the load-distribution curve. The other type of device used is illustrated in Fig 11(b). These are embedment gages, which are electrical strain gages placed in the shaft prior to casting the concrete. The gages indicate the strain in the shaft under various loadings. This value of strain, along with the deformation characteristics of the shaft, is used to develop the curve showing the distribution of load in a shaft with depth.

Lateral Pressure Gage

The device developed to measure the normal pressure between the soil and the concrete of the drilled shaft at the time of placing the concrete (see Fig 12) is a diaphragm-type pressure cell with strain gages affixed to the inside. The cell is fastened to the side of the drilled hole prior to

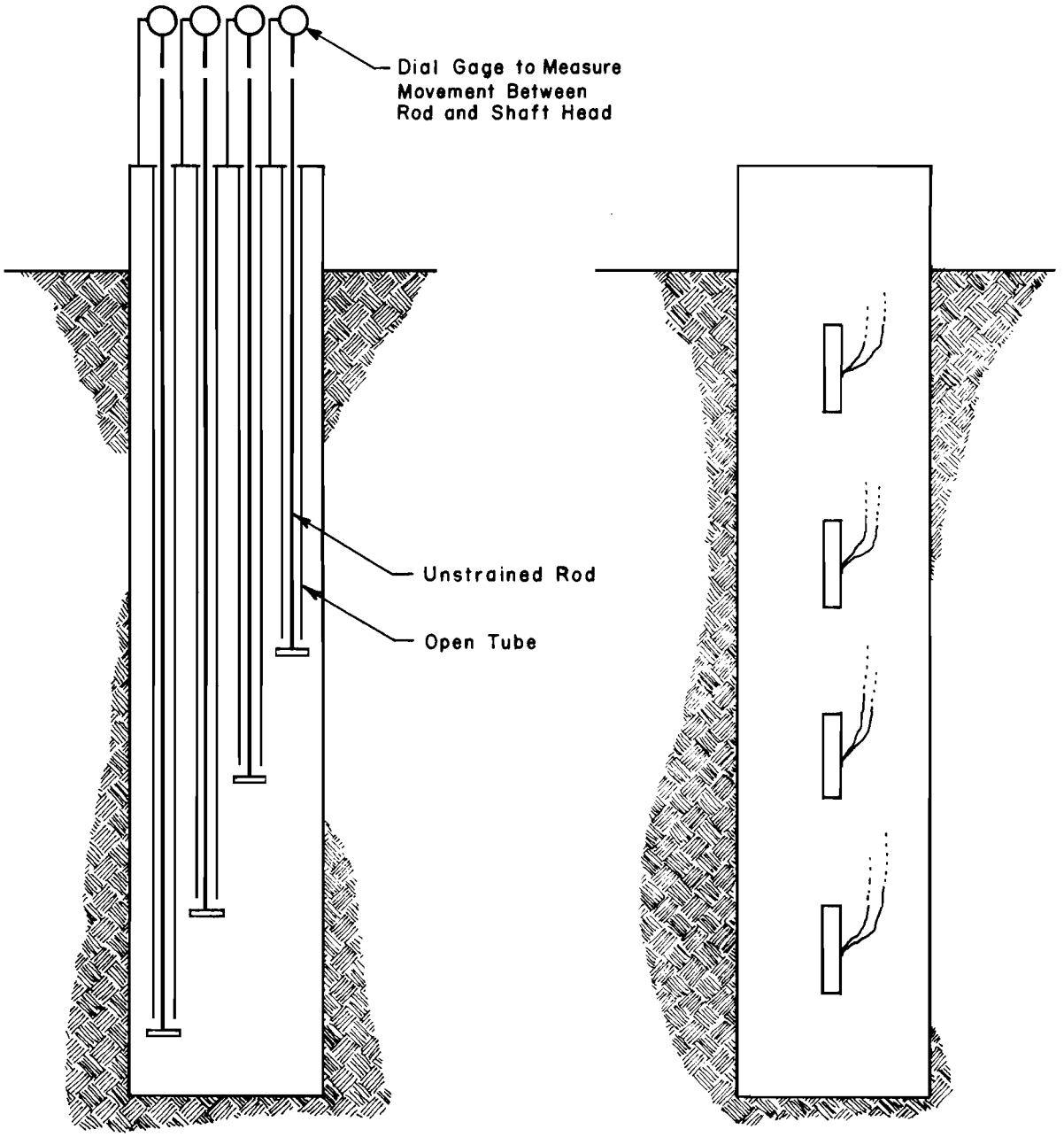

(a) Tell-tales (b) Embedment gages

Fig 11. Devices for determining axial load in a drilled shaft.

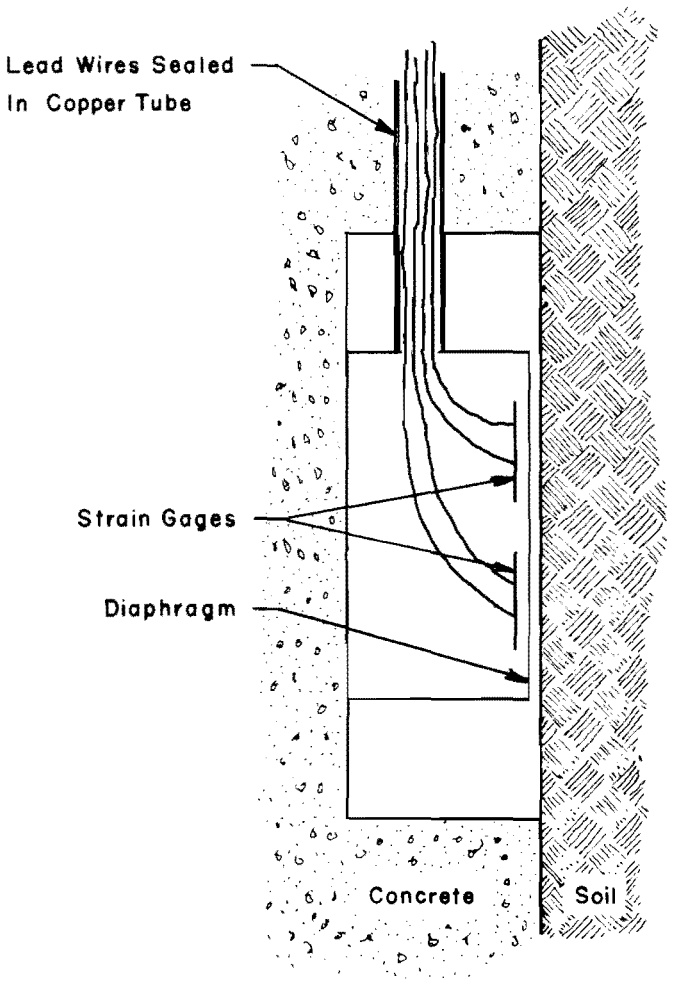

Fig 12. Pressure cell for measuring normal pressure between soil and concrete.

placing the cage of reinforcing steel, lead wires are brought to the surface, and readings are taken during and subsequent to the concrete pour. The measurement of soil pressure is a very difficult matter, and the complete success of these measurements is questionable. The details of the earth-pressure device will be discussed in a subsequent report.

Soil-Moisture Measurements

A nuclear device can be used successfully for measuring changes in soil moisture content. An aluminum tube is installed at the site to the desired measurement depth, and the moisture content determined by standard methods at the time of the installation. A nuclear probe is then lowered into the tube and an initial reading taken which is useful for calibration purposes. Subsequent readings can be taken at various times, as desired. This device has proved to be reasonably satisfactory, and a detailed report on its use will be forthcoming.

CHAPTER 5. RESULTS OF FIELD EXPERIMENTS

In previous studies of this problem and in the concept of this project, the use of large scale field studies has seemed essential. Thus, the plan is to test shafts at several locations in several different types of soil. Simple load-settlement tests can make important contributions to the problem. However, more complete information is needed, requiring the extensive instrumentation discussed in Chapter 4. The results of the tests on each site will be the subject of a research report. In order to develop instrumentation, loading equipment, and technique, a small experimental shaft was tested near Montopolis, Texas, as a precursor to the more complex tests (see Figs 13 and 14).

Soils Information

The soil at the Montopolis site may be summarized as follows:

From 0 to 3 ft - a stiff, dark grey clay (CH) with a few hair roots and some calcareous material. The water content of this clay is equal to its plastic limit, the unconfined compressive strength is about 2 ton/ft^2, and the strain at failure is from 1.5 to 4.0 percent.

From 3 to 6 ft - a hard, dark grey clay (CH) with some calcareous material. The water content is somewhat below its plastic limit, the unconfined compressive strength is from 3-10 tons/ft^2, and the strain at failure is about 1.4 to 2.0 percent.

From 6 to 10 ft - a grey and tan clay (CL) with calcareous material and a water content below the plastic limit. The unconfined compressive strength is between 3 and 7 tons/ft^2, and the strain at failure is from 0.8 to 1.6 percent.

From 10 to 17 ft - a tan clay (CL) with calcareous material. The water content is below its plastic limit and is believed to be very close to its shrinkage limit. The unconfined compressive strength is about 5 tons/ft^2, and the strain at failure is about 1 percent.

From 17 to 21 ft - a tan, sandy clay (CL).

These soil layers are illustrated in Fig 15.

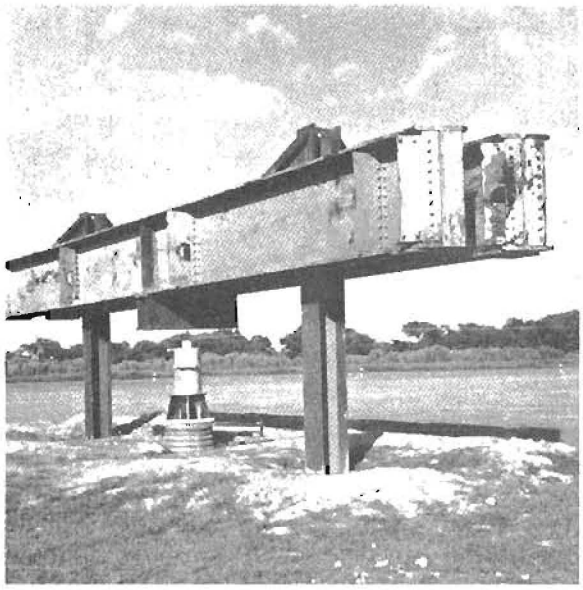

Fig 13. View of the Montopolis field test arrangement prior to loading.

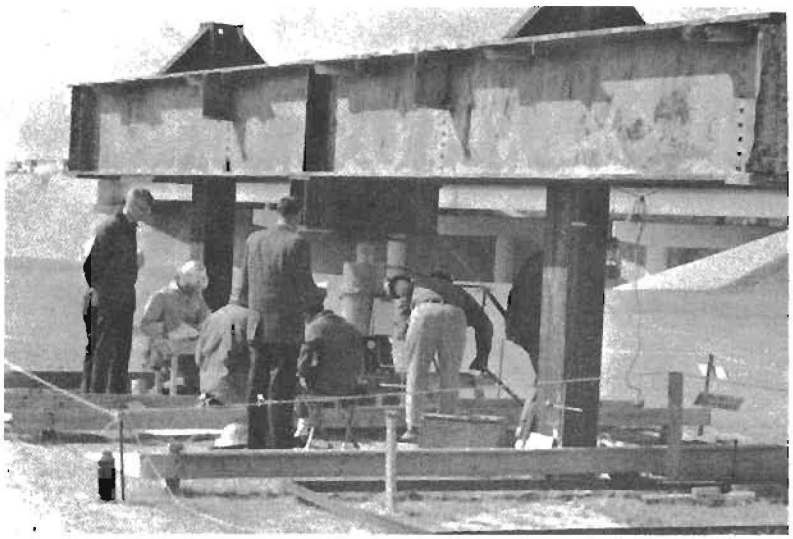

Fig 14. View of the Montopolis field experiment with loading test in progress.

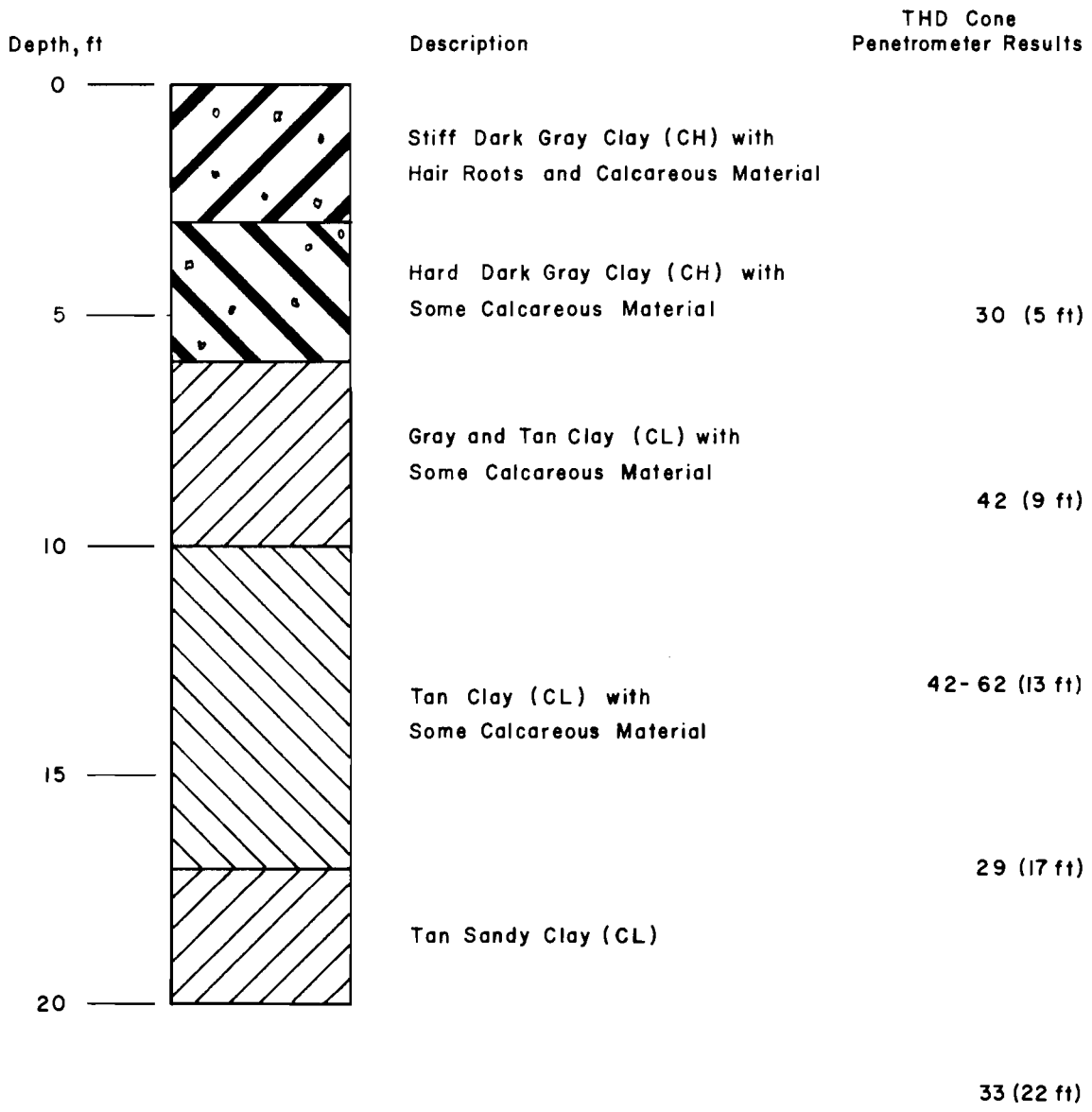

Fig 15. Soil profile for test site at Montopolis.

Instrumentation

Instrumentation for the measurement of the following was provided:

(1) axial loads at top and at three levels in the shaft,
(2) lateral earth pressures,
(3) temperature inside the shaft, and
(4) settlement.

Axial-Load Measurements. Both methods described previously were used to measure the axial loads in the shaft, namely, tell-tales and embedment gages.

The details of the assembly of the tell-tale system are shown in Fig 16(a). It consisted of unstrained rods or tubes, 1/2 in. in diameter, with a threaded end and an outer protective covering, 3/4 in. in diameter. A sleeve consisting of a 1-in.-diameter by 2-in.-high iron pipe was welded to a steel plate 3 in. in diameter and 3/8 in. thick. This steel plate with sleeve was screwed to the unstrained rod at the time of installation. The protective tube was slipped on to the unstrained rod and was kept 1/2 in. away from the steel plate by inserting a pin through the outer protective tube and inner unstrained rod near the top end. The space between the sleeve and the outer protective tube was filled with grease to prevent the entry of concrete between the inner rod and the protective tube, and the whole assembly was attached to the reinforcing cage with thin wires.

In all, two sets of tell-tale assemblies were used. Each set consisted of three different lengths, namely: 12 ft, 3 in.; 7 ft, 3 in.; and 5 ft, 3 in. For one set, unstrained rods were made from solid steel rod, and for the other set, unstrained tubes were made from 1/2-in. electric conduit with plugs inserted at each end. The plug at the lower end had a threaded projection to fit into the hole in the steel plate. The electric conduit was found to be more useful due to its light weight. Figure 16(b) shows a view of the top of the shaft with tell-tale projections.

Concrete embedment strain gages of the type PML-60, Polyester molded, of Japanese manufacture, were located at three different depths (see Fig 17) for measurement of axial strain. Four embedment strain gages were spaced equally at each depth, and additionally, two embedment gages were located at

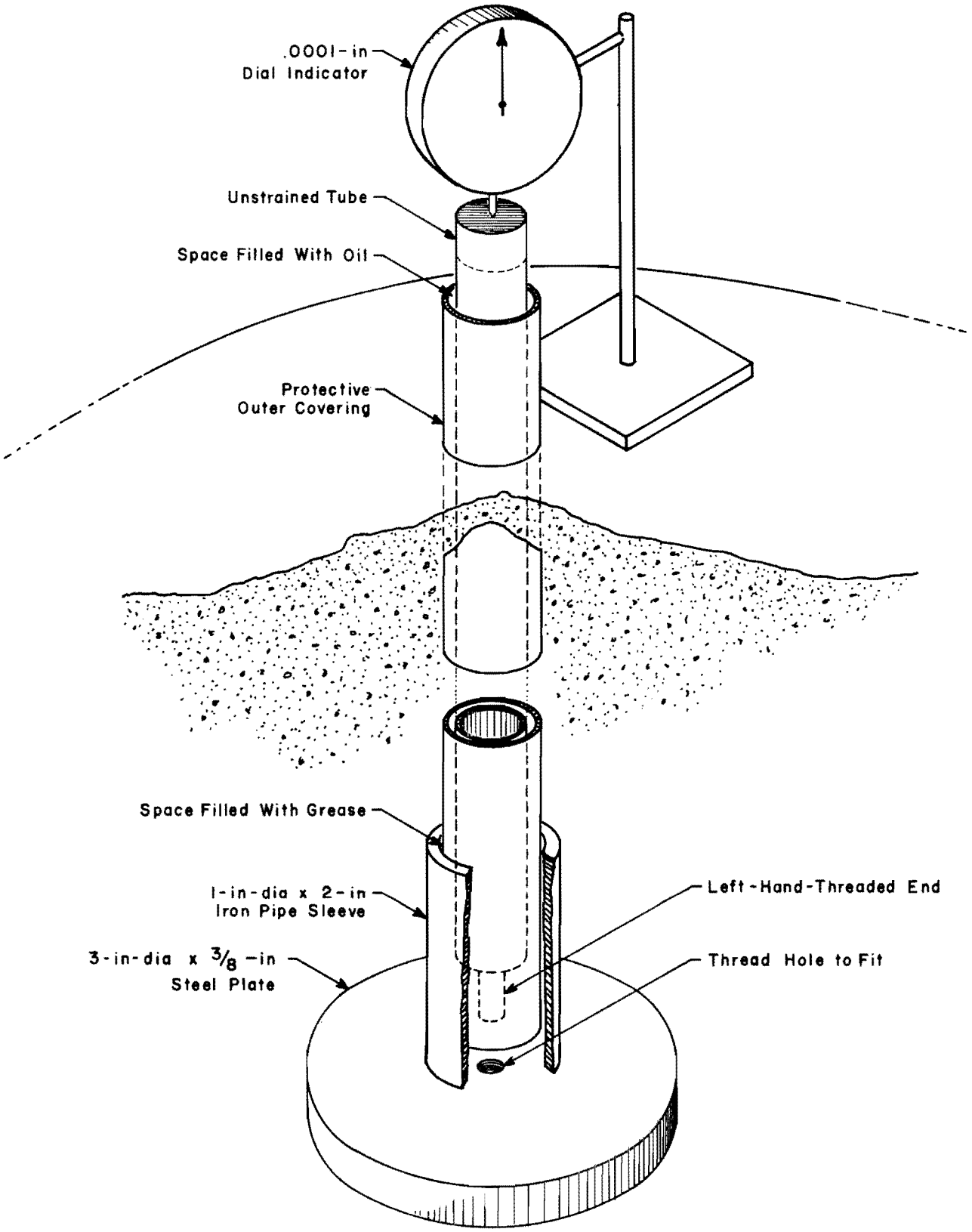

Fig 16(a). Details of the assembly of the tell-tale system.

Fig 16(b). View of tell-tales at top of shaft.

a depth of 6.8 ft to measure lateral strain. At each location one of the gages was placed in a concrete block of 3 X 7 X 1 in.

All embedment gages were used as a single active element in a Wheatstone bridge circuit. The "dummy" gage used was cast in a concrete cylinder and buried 6 ft in the soil near the test shaft. This dummy was used in the bridge circuit as the adjacent arm for temperature compensation.

A manual balance strain indicator was used for readout of all measuring circuits completed through a pair of ten-channel "switch and balance" units.

Electrical connections between the readout equipment and the embedment gages were made through four conductor, shielded cables of Belden type 8723. Each cable carried connections to two gages. The solder connections between the cable and gage leads were protected with "heat shrinkable" tubing and coated with rubber to metal cement.

This method of waterproofing was found to be inadequate and a possible contribution to the low electrical leakage resistance encountered after a period of several weeks.

Location of the "dummy" strain gage in an "unstrained" environment within the shaft would also provide better temperature compensation for measuring circuits.

Lateral-Earth-Pressure Measurements. Details of the diaphragm-type pressure cells used to measure lateral earth pressure and the method of installation are described in a separate report, and only a brief description of the cells is given here. The locations of these cells are shown in Fig 17.

The lateral-earth-pressure cells were developed by project personnel at The University of Texas for use on this project. The cells were machined from a berillium-copper alloy to provide a thin diaphragm sensing area. This sensing area was instrumented with Baldwin Lima Hamilton type FAES-4-150-1256, four arm, foil strain gages.

The full bridge configuration of this strain gage provided the necessary sensitivity and temperature compensation for use as a pressure transducer. The sealed transducer was provided with a copper-tubing fitting to accept the tubing for lead-wire protection to the surface. These gages were monitored with a manual balancing strain indicator through a special switch and balance unit which provided indicator zero and calibration check facility.

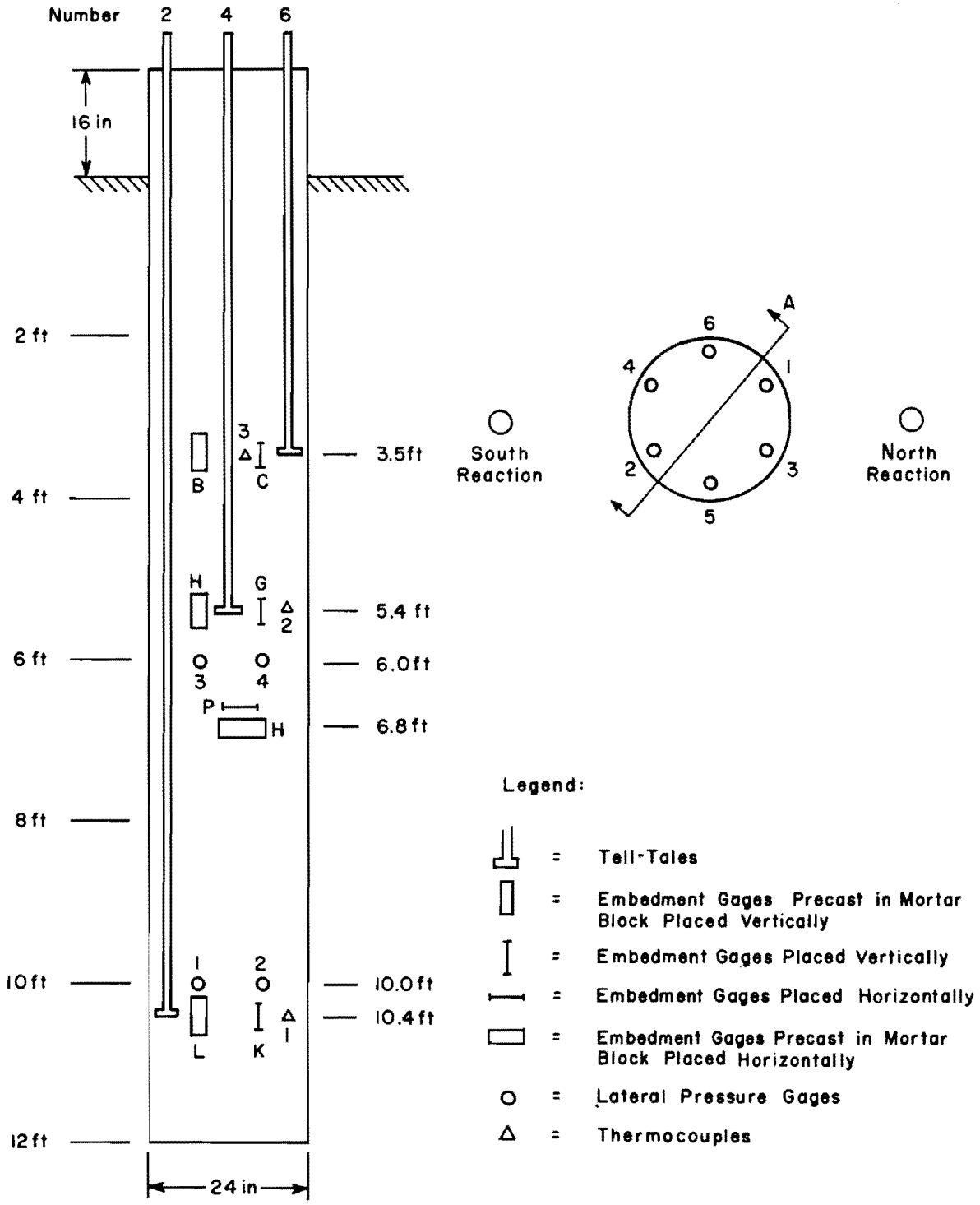

Fig 17. Locations of strain gages, tell-tales, lateral pressure gages, and thermocouples.

Temperature and Moisture Measurements. Thermocouples were installed in the test shaft to monitor the temperature variation. The locations of these are shown in Fig 17. The thermocouples were monitored with a Leeds and Northrop portable potentiometer.

Moisture measurements were taken from the soil samples obtained at the site location before test shaft installation. It was planned that a regular monitor of moisture be kept by using a "nuclear moisture" probe; however, due to a long delay in purchase and calibration of a "down hole" probe this device was not ready for use during the the testing at this site.

Loading Equipment

The head of the concrete shaft was capped with molding plaster in a manner to produce a horizontal plane bearing surface. A 1/2-in.-thick circular steel plate 24 in. in diameter was put on top of the shaft cap. This steel plate had six holes, each 1-1/2 in. in diameter, at locations corresponding to the tell-tale projections above the shaft head. A loading head (Fig 18) was used to transfer the load from the bottom of the jack to the top of the steel plate.

A jack of 400-ton capacity was used. Half-inch-thick plywood was put at the top of the hydraulic ram to provide uniform contact. Steel spacer plates of 1-in. thickness were also used between the plywood and the box that was fixed across the reaction beams. Reaction beams consisted of two 36 WF sections.

Load Tests

In all, eight axial-load tests were carried out at this site. The date of testing and type of tests were as shown in Table 1.

Tests 1 through 3 were conducted to evolve a suitable loading procedure and to determine the reliability and repeatability of the instrumentation used in the shaft. The load was applied in 10-ton increments and held for 30 min. During that time readings were taken for all shaft instrumentation at intervals of 1/2, 4, 8, 15, and 25 min for each loading increment. On completion of readings for a 40-ton load, the shaft was unloaded immediately to a zero load, and additional readings were then made for a period of 30 min.

Fig 18. View of loading head, settlement gages, and tell tales.

TABLE 1. SCHEDULE OF TESTING

Test No.	Date	Incremental Time, min	Maximum Load Applied, tons
1	Oct. 5, 1966	30.0	40
2	Oct. 19, 1966	30.0	40
3	Oct. 21, 1966	30.0	40
4	Feb. 2, 1967	30.0	20
5	Feb. 3, 1967	30.0	160
6	Mar. 15, 1967	15.0	160
7	Mar. 22, 1967	2.5	150
8	Mar. 22, 1967	2.5	150

Test 4 was carried out a day before the full-scale load test to check out the instrumentation. Tests 5 and 6 were full-scale load tests. The failure load, found to be 160 tons, here refers to the ultimate load at which the hydraulic loading jack had to be pumped continuously to maintain the load. The loading procedure was essentially the same as in earlier tests except that the time interval between two loadings was 15 min for Test 6.

Tests 7 and 8 were run according to the "Quick Test Load Method" of the Texas Highway Department. Test 8 was started one hour after the unloading for Test 7.

The load-settlement curves for Tests 5 through 8 are shown in Fig 19.

Discussion of Results

Since this test shaft was primarily meant to develop suitable instrumentation, test procedure, and related features, the data were not analyzed rigorously. However, the results of Tests 6, 7, and 8 were very similar. A typical load distribution in the shaft is shown in Fig 20. The load transferred to the tip of the shaft was about 18 to 30 percent of the failure load applied at the top.

Temperature variation created considerable drift in the strain gage readings, but it is felt that the provision of one dummy strain gage at each location of active strain gages will reduce this drift. Further, equal spacing of strain gages at each location should reduce the effect of eccentricity in loading.

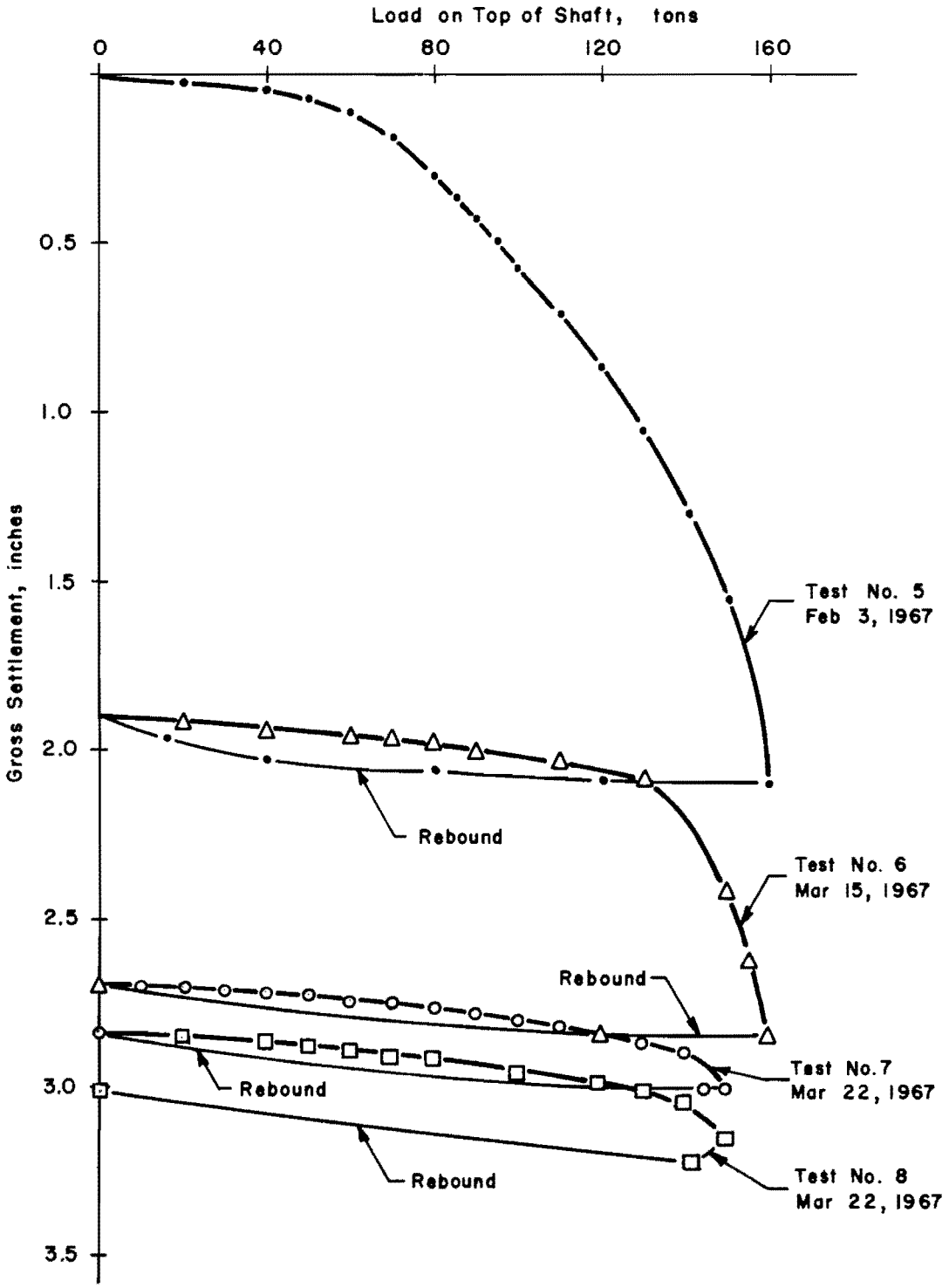

Fig 19. Load-settlement curves at Montopolis site.

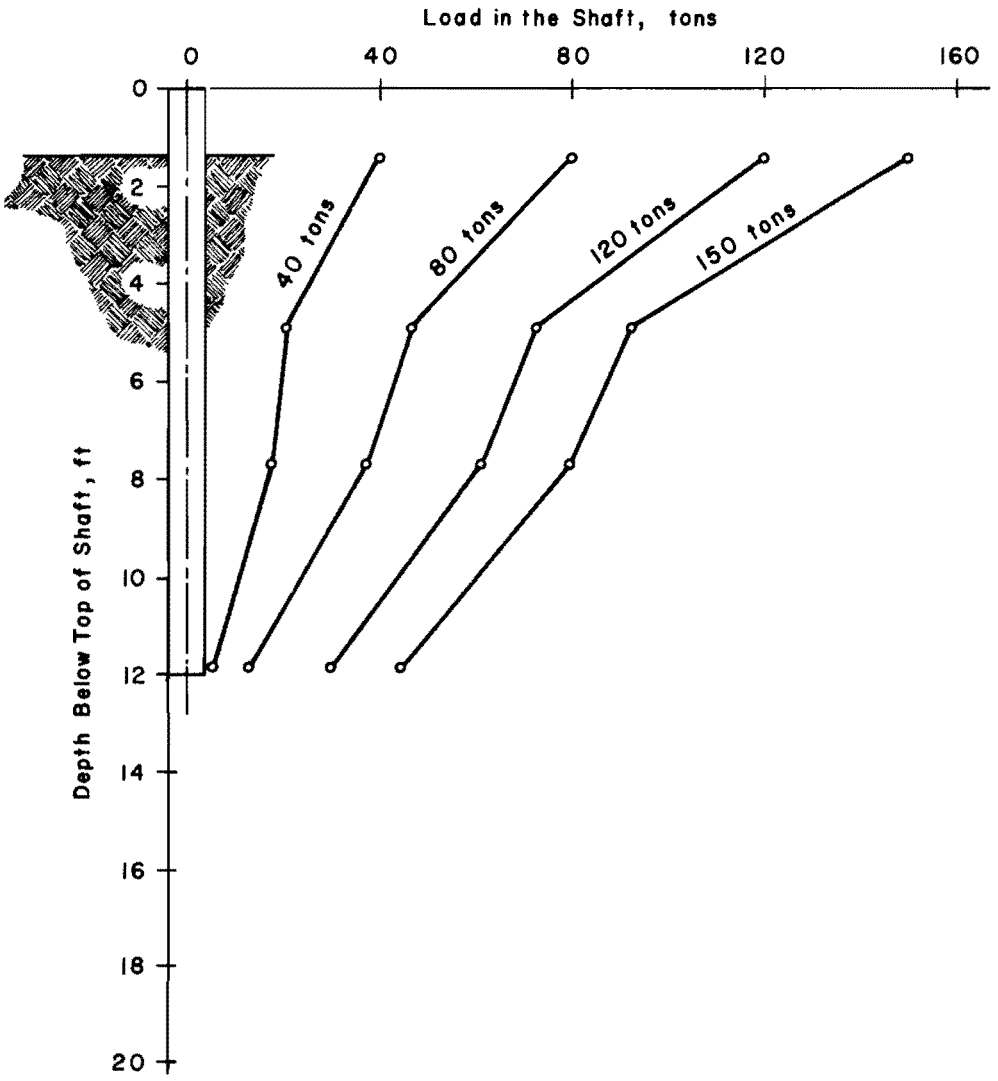

Fig 20. Typical load-distribution curves for Test 7 at Montopolis site.

CHAPTER 6. PRELIMINARY METHOD FOR COMPUTING ULTIMATE CAPACITY OF A DRILLED SHAFT

The aim of the research reported herein is to develop methods for computing the behavior of drilled shafts in a wide variety of soils and for various environmental conditions. This goal cannot be realized until a considerable amount of data is obtained to provide reasonable predictions of load-transfer curves for the sides of the shaft and of a load-settlement curve for the tip of the shaft.

However, a preliminary method of computing the ultimate capacity of a drilled shaft should be useful as an interim guide. The method can be expanded and improved as results of tests become available. The weakness of this preliminary method is, of course, that the settlement corresponding to the ultimate capacity is unknown. Further, the method is based only on the preliminary results in this report and is limited to soil types similar to those at the Montopolis site.

The computation of the ultimate load on a drilled shaft proceeds in two parts: computation of load carried (1) by the side of the drilled shaft and (2) by the tip of the drilled shaft. This method assumes no interaction between the tip and the sides of the shaft in carrying load, an assumption which is not strictly correct but is sufficiently valid for the present purposes. Future research in this project will consider this interaction.

Computing Load Capacity Along the Side of a Drilled Shaft

The load carried by the side of the drilled shaft can be estimated by using the modified shearing resistance of the soil. The procedure involves dividing the shaft into a number of increments, calculating the load capacity for each increment, and summing this load. Specifically, the procedure is as follows:

(1) Using the modified shearing resistance of the soil, compute the load carried by each increment along the drilled shaft by using the following expression:

$$\Delta R_i = \Delta \bar{A}_i c_i \alpha_i \tag{13}$$

where

ΔR_i = shaft side resistance at the i^{th} increment,

$\Delta \bar{A}_i$ = area of the side of the drilled shaft in contact with the soil at the i^{th} increment,

α_i = the minimum value of α at the i^{th} increment,

c_i = shearing resistance of an undisturbed sample at the i^{th} increment.

(2) The estimated load carried by the side of the drilled shaft is equal to the sum of the shaft side resistance of each increment. Thus,

$$R = \sum_{i=1}^{M} \Delta R_i = \sum_{i=1}^{M} \Delta \bar{A}_i c_i \alpha_i \tag{14}$$

where M is the total number of increments.

The Montopolis shaft, 2 ft in diameter and 12 ft long, is used in the following example of this procedure. The moisture content and unconfined compression strength variations are shown in Fig 21 where Curve A is the best second degree least squares fit to twelve feet for moisture content, and Curve B is the best fit for unconfined compression strength. The water-cement ratio of the concrete was 0.6.

Undisturbed samples were tested for moisture migration at depths of 3, 6, 8, 9, 11, and 13 ft. The overburden pressure applied during the curing periods for samples at 8, 9, 11, and 13 ft was 10 psi, while an overburden pressure of 5 psi was used for the samples taken at 3 and 6 ft. These overburden pressure values were taken to represent the approximate lateral pressures exerted by the concrete on the soil at the various levels as computed by the ACI formula for lateral concrete pressure on form work (Ref 6). Actual lateral pressure variations will be discussed in a later report. The moisture content versus distance from the interface at each depth obtained from these tests is shown in Fig 22, and the average moisture-content increase in the first inch for various water-cement ratios is given in Table 2. Moisture migrated up to 1-1/2 in. into the soil, thus decreasing the shear strength in that region near the interface.

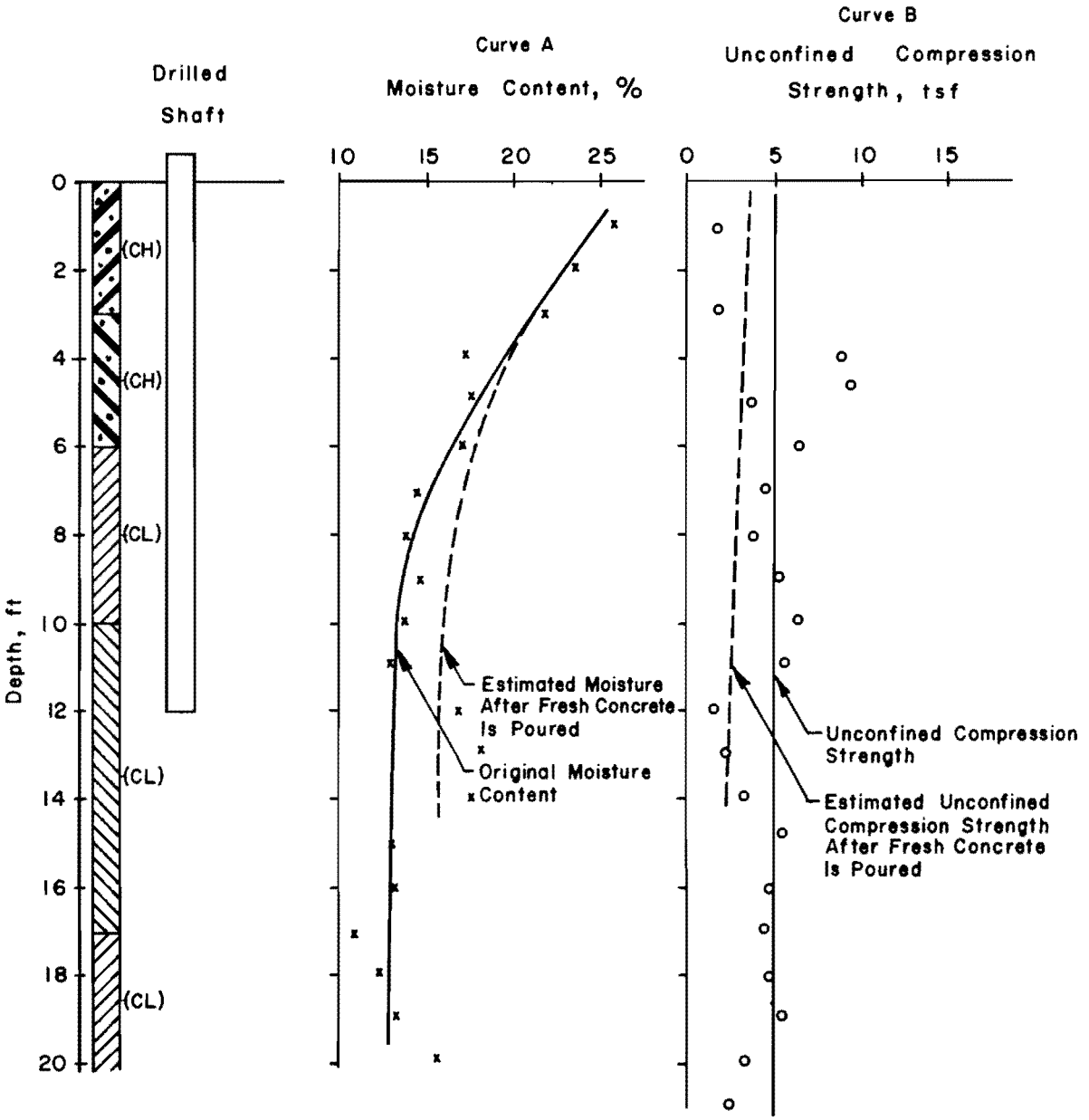

Fig 21. Estimated moisture and shearing resistance of soil at various depths.

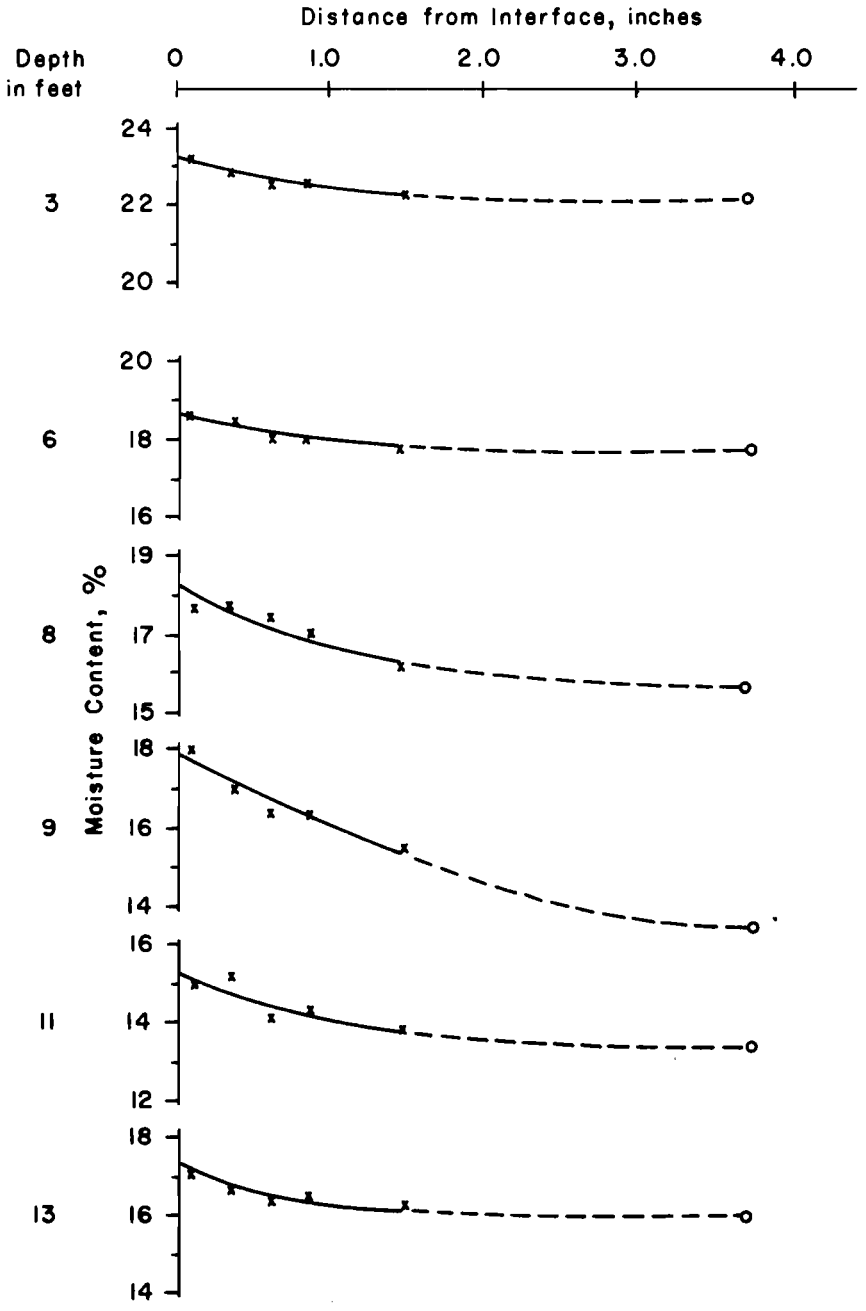

Fig 22. Variation in moisture content with distance from interface.

TABLE 2. MOISTURE MIGRATION ON UNDISTURBED SAMPLES

Depth ft	Water-Cement Ratio = 0.6		Water-Cement Ratio = 0.7		Water-Cement Ratio = 0.8	
	Initial Moisture Content	Δw Average Increase in First Inch	Initial Moisture Content	Δw Average Increase in First Inch	Initial Moisture Content	Δw Average Increase in First Inch
3	27.10	-	23.15	0.44	21.60	1.30
6	18.00	0.37	17.28	2.23	18.35	2.60
8	16.00	1.61	16.10	2.24	16.00	3.28
9	13.70	3.19	13.10	3.42	13.70	4.88
11	13.82	2.08	13.82	2.04	13.80	2.33
13	15.00	1.99	14.30	2.38	14.95	3.24
15	-	-	-	-	12.70	-

Direct shear tests to study the shearing plane developed at various distances from the interface were conducted on mortar-soil samples taken from the same depths and tested at the same overburden pressures (the 3-ft sample was omitted). The results of these tests are plotted in Fig 23.

Figure 23 clearly indicates that the zone of weakest soil occurs at about 1/4 in. from the interface. Hence, the soil in this zone will have its maximum shearing resistance mobilized first, and failure will occur at approximately 1/4 in. from the interface.

Assuming the shearing resistance of the soil is fully developed along the drilled shaft, the total load on the side of the drilled shaft is equal to R. The computation of the load is shown in Table 3, with the computed load being 104.5 tons.

The actual side load obtained from analyzing the results of Test 6 was 106 tons. The side load was separated from the total load applied at the top of the shaft by the use of instrumentation along the shaft. For this test, the agreement between computed and experimental values of the side load was very good.

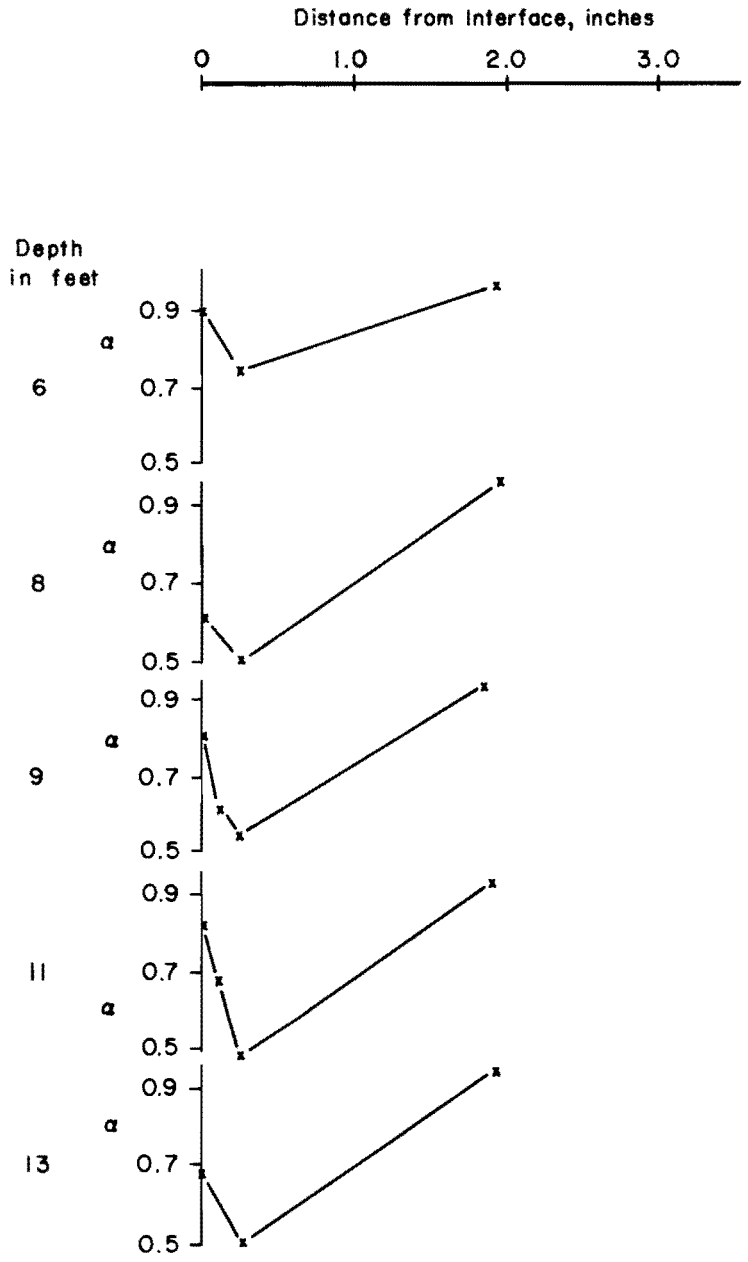

Fig 23. Variation in α with distance from interface.

TABLE 3. LOAD COMPUTATION

Depth Interval ft	c TSF	α	c α TSF	ΔA ft^2	ΔS tons
0-6	1.70	0.79	1.34	38.46	51.5
6-8	2.10	0.52	1.09	12.82	15.6
8-9	2.55	0.53	1.35	6.44	7.8
9-11	3.48	0.50	1.74	12.82	19.9
11-12	2.50	0.51	1.28	6.44	9.7
Total load carried by side of the drilled shaft					104.5

If no reduction is made for loss in shear strength due to moisture migration, the computed capacity of the side of the drilled shaft is 189 tons. Considering moisture migration, however, the capacity is 104.5 tons. Thus, it is important to take into account the moisture migration and consequent strength loss.

Computing Load Capacity at the Tip of a Drilled Shaft

The load capacity of the tip of a drilled shaft can be computed by use of bearing-capacity theory. Assuming the unit weight of concrete is the same as the unit weight of soil, the following equation can be used to compute the load capacity of the tip:

$$Q_B = N_c A_B c_B \tag{15}$$

where

Q_B = ultimate tip load,

N_c = bearing-capacity factor at the tip of the shaft,

A_B = area of the tip of the shaft,

c_B = modified shearing strength of soil at the tip of the shaft.

Formulas for the bearing-capacity factors have been presented by a number of authors. The method proposed by Skempton (Ref 5) is well accepted for clay soils at the present time. For a circular footing, Skempton's recommendations for N_c are shown in Fig 24.

Perhaps the most difficult problem in determining the ultimate bearing capacity of the tip of the drilled shaft is ascertaining the soil shear strength. While it is known that some softening will occur, the amount of moisture migration and shear strength loss is unknown at present.

In this analysis it is assumed that the modified shear strength is midway between the initial shear strength and the fully softened shear strength; thus, a value of 1.88 TSF will be employed (see Table 3). Substituting into Eq 15

$$Q_B = (9)(\pi)(1.88)$$

$$= 53 \text{ tons} . \qquad (16)$$

The bearing-capacity factor $N_c = 9$ is estimated from Fig 24.

The measured load carried by the tip of the shaft was 54 tons, as determined from results of Test 6. This value agrees extremely well with the computed tip load of 53 tons.

Actually, the moisture content of the soil around the drilled shaft changes with time, that is, with periods of heavy and prolonged rainfall or periods of severe drought. As a consequence, changes in the soil properties and in the load transfer characteristics will occur. Therefore, the computations shown are valid only for a certain period of time after the shaft has been constructed. The nature of the adjustments that will have to be made in computation procedures to account for future precipitation variations is at present unknown.

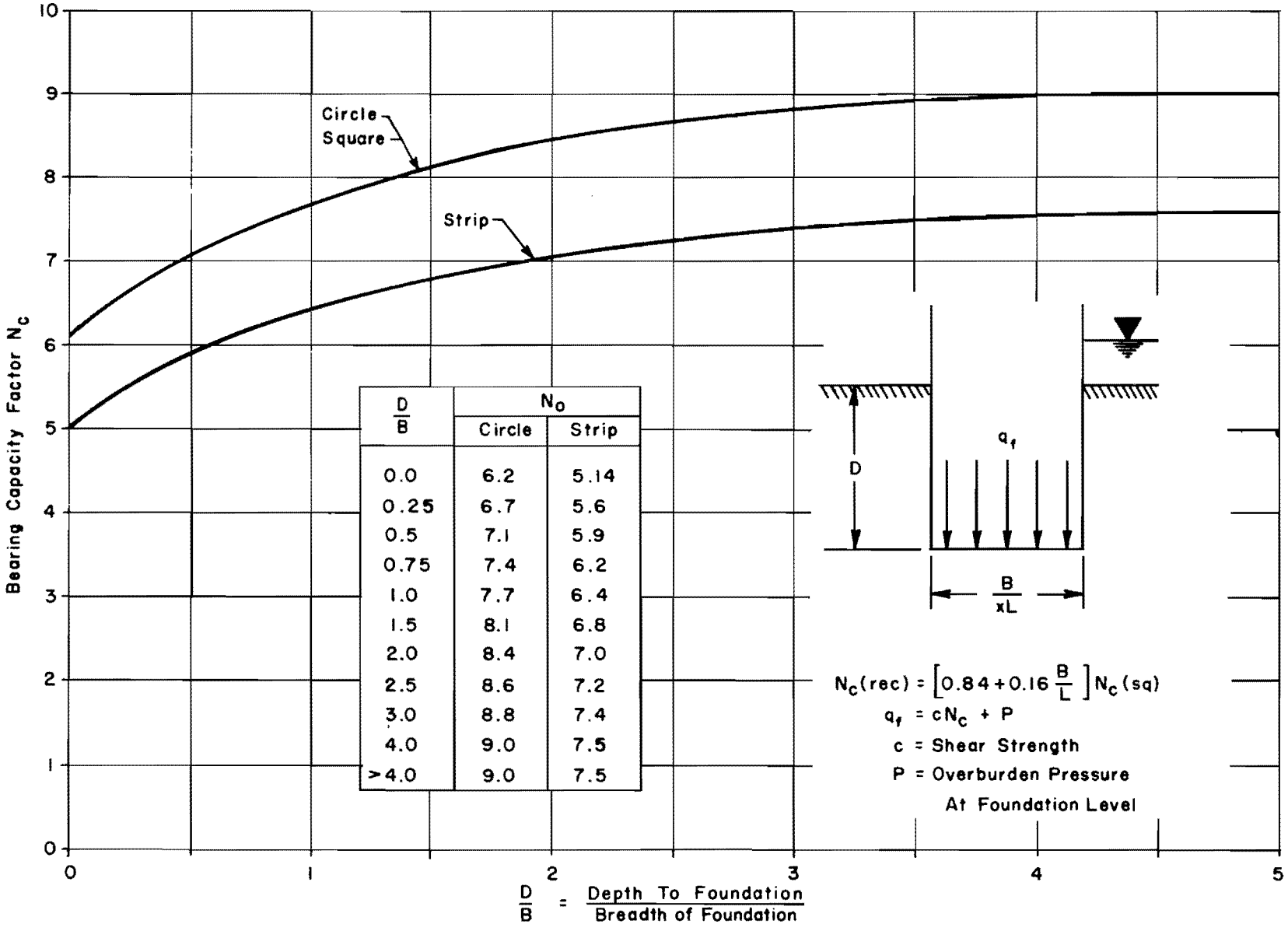

$\frac{D}{B}$	N_o	
	Circle	Strip
0.0	6.2	5.14
0.25	6.7	5.6
0.5	7.1	5.9
0.75	7.4	6.2
1.0	7.7	6.4
1.5	8.1	6.8
2.0	8.4	7.0
2.5	8.6	7.2
3.0	8.8	7.4
4.0	9.0	7.5
>4.0	9.0	7.5

Fig 24. Bearing capacity factors for foundations in clay (ϕ = 0) (from Ref 5).

CHAPTER 7. SUMMARY AND RECOMMENDATIONS

The problems of designing drilled shafts are complex, involving a variety of factors with a spatial and time variability. Accurate determination of the load-carrying capacity of drilled shafts is practically impossible because so many effects are not well defined. In particular, the load-settlement and the load-distribution curves for shafts cannot be easily determined. Superposed on the requirements for a particular shaft are the wide variety of soil and environmental conditions in which such shafts must be constructed.

The physical requirements and the testing program described herein are vital to the development of a rational procedure for designing drilled shafts. This is the first in a series of reports planned to describe the important parts of the program. The others include:

(1) a report describing the development of instrumentation and the study of lateral earth pressure against shafts,

(2) a study and report on the soils aspects of the problem, including the problems of soil-concrete interaction and the measurement of shear strength,

(3) a report describing the development of instrumentation for measuring moisture migration near drilled shafts,

(4) reports on a series of load tests on a full-sized shaft in San Antonio, Texas, to develop necessary load-distribution and load-settlement information for a particular location,

(5) reports on a second series of load tests on full-sized shafts in Houston, Texas, to study the same factors under different soils and environmental conditions,

(6) reports on an effort to combine all data developed in Items 1 through 5 into a preliminary design approach for drilled shafts considering as many factors as realistically possible, and

(7) a study of the problem in the light of the preliminary design approach to see what future investigations are desirable and how sensitive the proposed method is to various other factors.

It has been the purpose of this report to put the problems of designing drilled shafts in perspective and to develop the preliminary procedures which

will be used in subsequent phases. Several other reports will be forthcoming in the very near future as testing and analysis are completed.

REFERENCES

1. Reese, Lymon C., "Load Versus Settlement for an Axially Loaded Pile," Proceedings, Symposium on Bearing Capacity of Piles, Part 2, Central Building Research Institute, Roorkee, February 1964, pp. 18-38.

2. Seed, H. B. and Lymon C. Reese, "The Action of Soft Clay Along Friction Piles," Transactions, American Society of Civil Engineers, Vol 122, 1957, pp 731-764.

3. Coyle, Harry M. and Lymon C. Reese, "Load Transfer for Axially Loaded Piles in Clay," Journal of the Soil Mechanics and Foundations Division, American Society of Civil Engineers, Vol 92, No SM2, March 1966, pp 1-26.

4. Coyle, Harry M. and Ibrahim H. Sulaiman, "Skin Friction for Steel Pipes in Sand," Proceedings, American Society of Civil Engineers, Vol 93, No SM6, November 1967, pp 261-278.

5. Skempton, A. W., "The Bearing Capacity of Clays," Building Research Congress, Division I, Part III, 1951, pp 180-189.

6. "Recommended Practices for Concrete Formwork," Standards, American Concrete Institute, 1963, pp 347 - 363.